THE EFFECT OF PHYSICAL PROPERTIES OF THE ELP-COLLAGEN BASED
PATTERNED SURFACES ON CELL ATTACHMENT AND DEFORMATION


A THESIS SUBMITTED TO
THE GRADUATE SCHOOL OF NATURAL AND APPLIED SCIENCES
OF
MIDDLE EAST TECHNICAL UNIVERSITY


BY


EZGİ ANTMEN


IN PARTIAL FULFILLMENT OF THE REQUIREMENTS
FOR
THE DEGREE OF MASTER OF SCIENCE
IN
BIOLOGY


SEPTEMBER 2013

Approval of the thesis:

**THE EFFECT OF PHYSICAL PROPERTIES OF THE ELP-COLLAGEN BASED PATTERNED SURFACES ON CELL ATTACHMENT AND DEFORMATION**

submitted by **EZGİ ANTMEN** in partial fulfillment of the requirements for the degree of **Master of Science in Biology Department, Middle East Technical University** by,

Prof. Dr. Canan Özgen
Dean, Graduate School of **Natural and Applied Sciences**
                                    _____

Prof. Dr. Gülay Özcengiz
Head of Department, **Biological Sciences Dept., METU**
                                    _____

Prof. Dr. Vasıf Hasırcı
Supervisor, **Biological Sciences Dept., METU**
                                    _____

Assist. Prof. Dr. Utkan Demirci,
Co-Supervisor, **Harvard University, Boston, USA**
                                    _____

**Examining Committee Members:**

Prof. Dr. Gülay Özcengiz
Biological Sciences Dept., METU
                                    _____

Prof. Dr. Vasıf Hasırcı
Biological Sciences Dept., METU
                                    _____

Prof. Dr. Aykut Özkul
Virology Dept., Fac. Veterinary Med., Ankara University
                                    _____

Prof. Dr. Musa Doğan
Biological Sciences Dept., METU
                                    _____

Assoc. Prof. Dr. Tülin Yanık
Biological Sciences Dept., METU
                                    _____

**Date:**         04.09.2013

**I hereby declare that all information in this document has been obtained and presented in accordance with academic rules and ethical conduct. I also declare that, as required by these rules and conduct, I have fully cited and referenced all material and results that are not original to this work.**

Name, Last Name: Ezgi ANTMEN

Signature            :

**ABSTRACT**


**THE EFFECT OF PHYSICAL PROPERTIES OF THE ELP-COLLAGEN BASED PATTERNED SURFACES ON CELL ATTACHMENT AND DEFORMATION**



Antmen, Ezgi
M.Sc., Department of Biology
Supervisor: Prof. Dr. Vasıf Hasırcı
Co-Supervisor: Assist. Prof. Dr. Utkan Demirci

September 2013, 67 Pages


Cell and substrate interactions are important in tissue engineering products especially on the behavior of the cells such as adhesion, migration, proliferation, and differentiation. These have been widely studied using substrates with different physical, chemical, and mechanical properties and form.

In this study, elastin-like recombinamers (ELRs) were used blended with collagen or only collagen as the surface material. The ELR used in this study has Valine-Proline-Glycine-X-Glycine aminoacid sequences in its primary structure as the repeating sequence. Collagen was used because it is a biodegradable and biocompatible polymer. The films used for this study were designed to have micropillar covered surfaces with the pillar dimensions involving 4 regions covered with 8x8 µm² and 16x16 µm² pillars separated by either 4 or 8 µm gaps with a height of 5 µ. Saos-2 human osteosarcoma cell line was used to study cell behavior (proliferation, adhesion and conformational change) on these films. Films were observed after 1 day and 14 days of culture by using fluorescence microscopy and SEM and ALP activity of the cells on the micropillar covered surfaces were determined by alkaline phosphatase (ALP) assay after 14 days of culture. Deformation extent and fraction of deformed cells were measured.

In terms of adhesion, there was no significant difference in between the different surfaces as a result of ELR presence whereas the micropillar dimensions affected the number of cells and cell numbers were the least at area B which has the lowest pillar size with highest gap (8x8 µm², gap 8 µm) where it was higher for unpatterned surfaces on the 1st day of the culture. Also there was no consistent difference between the three types of films considering the contribution of ELR to the stiffness of the surface. For the 14th day of the culture, it was observed that there is almost no cell on the micropillar surfaces but there were a number of cells on the middle of the films which has no micropillar probably due to the deformation in the micropillar geometries of the films stored in PBS. In terms of ALP concentration, results showed that the highest ALP activity on the films with the highest ELR ratio and higher ALP activity with the cells on the B area but the highest activity with cells on TCP. Lastly, in terms of conformational changes of the cells, it was observed that cells and their nuclei are deformed on the micropillar covered surfaces on all types of films. ELR and collagen content

of the films did not seem to affect nuclei deformation. However, pillar placement and dimensions seem to be effective on the nuclei shapes that nuclei of the cells fall in the gaps when the gaps are large enough and when the gaps were smaller, nuclei were observed mostly on the pillar surfaces instead of the gaps. Moreover, there was a consistency between the nucleus and cell deformations in terms of shape. Also there was no cell deformation on the smooth, unpatterned surfaces and the reason of the deformations was the pillars on the film surfaces. In deformation quantification analysis, nuclei deformation frequency, nuclei circularity and nuclei perimeter showed no significant difference between the different films with changing ELR contents. However, considering the pillar dimensions, the highest deformation frequency was on the smallest pillar with largest gap, the least circularity meaning the highest deformation can be seen for the design B (8x8 µm², gap 8 µm) and the highest perimeter for the nuclei was for areas having the highest pillar gaps as area B (8x8 µm², gap 8 µm) and D (16x16 µm², gap 8 µm).

# ÖZ

## ELASTİN BENZERİ POLİMER (ELP) VE KOLLAJENDEN YAPILMIŞ DESENLİ YÜZEYLERİN FİZİKSEL ÖZELLİKLERİNİN HÜCRE TUTUNMASI VE DEFORMASYONU ÜZERİNDEKİ ETKİSİ

Antmen, Ezgi

Yüksek Lisans, Biyoloji Bölümü

Tez Yöneticisi: Prof. Dr. Vasıf Hasırcı

Ortak Tez Yöneticisi: Yrd. Doç. Dr. Utkan Demirci

Eylül 2013, 67 sayfa

Doku mühendisliği ürünlerinde hücre ve yüzey etkileşimlerinin özellikle tutunma, göç etme, çoğalma ve farklılaşma gibi hücre hareketleri üzerindeki etkisi önemlidir. Bu etkiler farklı fiziksel, kimyasal ve mekanik özelliklere ve formlara sahip yüzeyler kullanılarak yaygın bir şekilde incelenmiştir.

Bu çalışmada, yüzey malzemesi olarak kollajenle çaprazlanmış elastin benzeri rekombinant polimerler (ELRs) ya da sadece kollajen kullanılmıştır. Bu çalışmada kullanılan ELR'nin birincil yapısında Valin-Prolin-Glisin-X-Glisin olarak tekrar eden amino asit dizileri bulunmaktadır. Kollajen biyouyumluluk ve bozunma özelliklerinden dolayı kullanılmıştır. Bu çalışmada kullanılan filmler 4 veya 8 μm aralıklarla ve 5 μm uzunluğunda 8x8 μm$^2$ veya 16x16 μm$^2$ boyutlarında mikro sütun kaplı yüzeyler olarak tasarlanmıştır. Bu filmler üzerinde hücre davranışlarını (çoğalma, tutunma, ve yapısal değişiklik) incelemek için Saos-2 insan osteosarkoma hücre hattı kullanılmıştır. Filmler hücre kültürünün 1. ve 14. günlerinde floresans mikroskobu ve taramalı elektron mikroskobu kullanılarak incelenmiş ve hücre kültürünün 14. gününde alkalin fosfataz (ALP) miktar tahlili yapılmıştır. Deforme olmuş hücrelerin deformasyon derecesi ve oranı ölçülmüştür.

Hücre tutunması bakımından, hücre kültürünün birinci gününde incelenen, mikro sütunlar hücres sayısını etkilemiş ve hücre sayısı mikro sütun boyutları en az, sütun aralıkları en çok olan B alanında (8x8 μm$^2$, 8 μm) diğer alanlara göre daha fazla ve desensiz yüzeyde en fazla iken, ELR oranının değiştiği farklı filmlerde belirgin bir hücre sayısı değişimi yoktur. Ayrıca ELR'nin yüzey sertliğine katkısı dikkate alındığında üç film çeşidi arasında tutarlı bir değişiklik yoktur. Hücre kültürünün 14. gününde, mikro sütunlu yüzeylerde hemen hemen hiç hücre olmadığı ve dilmlerin desensiz orta kısımlarında bir miktar hücre olduğu görülmektedir. Buna filmlerin tuzlu fosfat tamponu (PBS) içerisinde tutulduğu için sütun şekillerinde oluşan bozulmalar sebep olmuş olabilir. ALP aktivitesi açısından, sonuçlar en fazla ALP miktarının en fazla ELR oranına sahip filmlerde olduğunu ve diğer alanlara göre B alanında daha fazla ALP miktarı ve doku kültür kabında (TCP) en fazla ALP miktarı olduğunu göstermiştir. Son olarak, hücre yapısı değişiklikleri açısından, hücre ve çekirdekleri mikro sütun kaplı tüm film çeşitlerinde şekil bozuklukları göstermiştir. Filmlerin ELR ve kollajen içeriğinin hücre çekirdeklerindeki şekil bozukluklarını etkilemediği

görülmüştür. Ancak, sütun yerleşimi ve boyutlarının hücre çekirdeği şekil bozuklukları üzerinde etkili olduğu görülmüş ve sütunlar arasındaki boşluklar yeterince büyük olduğunda hücre çekirdeklerinin boşluklara düştüğü ve boşluklar daha küçük oduğunda çekirdeklerin boşluklar yerine daha çok sütun yüzeyleri üzerinde olduğu gözlenmiştir. Dahası, şekil yönünden hücre ve çekirdek bozulmaları arasında bir tutarlılık vardır. Ayrıca desensiz, düz yüzeylerde hücre bozulması yoktur ve bozulmaların sebebi film yüzeylerindeki mikro sütunlardır. Bozulma miktar analizlerinde, çekirdeklerin bozulma sıklığı, çekirdeklerin daireselliği ve çekirdeklerin çevre uzunluğu değişen ELR içeriğine sahip farklı filmlerde belirgin bir değişiklik göstermemiştir. kompozisyonlar arasında anlamlı bir fark gösterdi. Ancak, sütun boyutları dikkate alındığında, en yüksek çekirdek bozulma sıklığı en büyük sütun aralığına sahip en küçük sütun boyutlarında, en fazla bozulmayı ifade eden en küçük çekirdek daireselliği B alanında ve en büyük çekirdek çevre uzunluğu en fazla sütun aralıklarına sahip B ve D alanlarındadır.

**Anahtar kelimeler:** Mikrodesen, sütun, elastin benzeri rekombinant polimer, kollajen, polimerik filmler, bozulma, hücre çekirdeği, hücre-yüzey etkileşimleri

**Dedicated to My Big Family**

# ACKNOWLEDGEMENTS

# TABLE OF CONTENTS

# LIST OF FIGURES

xvi

# LIST OF TABLES

# LIST OF ABBREVIATIONS

| | |
|---|---|
| 2D | Two Dimensional |
| 3D | Three Dimensional |
| BSA | Bovine Serum Albumin |
| Col | Collagen |
| DAPI | 4', 6-diamidino-2-phenylindole |
| DHT | Dehydrothermal |
| DMSO | Dimethyl Sulfoxide |
| ECM | Extracellular Matrix |
| *E.coli* | *Escherichia coli* |
| ELP | Elastin Like Polymer |
| ELR | Elastin Like Recombinamer |
| FBS | Fetal Bovine Serum |
| FITC | Fluorescein Isothiocyanate |
| g | gram |
| Gly | Glycine |
| h | hour |
| ITT | Inverse Transition Temperature |
| HAc | Acetic Acid |
| min | minute |
| mg | milligram |
| mm | millimeter |
| mL | milliliter |
| nm | nanometer |
| kDa | kilo Dalton |
| M | Molarity |
| mM | millimolar |
| Na | Sodium |
| NaCl | Sodium Chloride |
| NaH2PO4 | Sodium phosphate monobasic |
| Na2HPO4 | Sodium phosphate dibasic |
| PBS | Phosphate Buffer Saline |
| PDMS | Poly(dimethylsiloxane) |
| PEG | Polyethylene Glycol |
| Pen/Strep | Penicillin/Streptomycin |
| PGA | Poly(glycolic acid) |
| PLA | Poly(lactic acid) |
| PLGA | Poly(Lactic Acid-co-Glycolic Acid) |
| PLLA | Poly(L-Lactic Acid) |
| SDS-PAGE | Sodium Dodecyl Sulphate- Polyacrylamide Gel Electrophoresis |
| SEM | Scanning Electron Microscopy |
| TCPS | Tissue Culture Polystyrene |

| | |
|---|---|
| Tt | Transition Temperature |
| UV | Ultra Violet |
| UXL | Uncrosslinked |
| v/v | volume/volume |
| w/v | weight/volume |
| μm | micrometer |

# CHAPTER I

# INTRODUCTION

## 1.1 Cell and Biomaterial Interactions

Cell and biomaterial interactions have a great importance in the performance of a biomaterial designed as an implant or a tissue engineering product. Surface topography of the substrate materials and the interaction between the membrane and the substrates are involved in this step and cytoskeleton and plasma membrane are intensely involved in these relations. These are expected to influence cell attachment, migration, metabolism, proliferation and even differentiation. In 1912, Harrison was the first to show the effect of solid supporting materials on cell movement and morphogenesis by using spider web as the substrate. He realized that the cells were changing their shape and movement in accordance with the spider web organization. Similar observations were made by his group in those times. In 1947, Paul Weiss showed that cells move and migrate through contact guidance which meant the cells responded to the substrate topography by aligning and elongating in the direction of the topographical features. Later, in 1964 Curtis and Varde used topography to control cell behavior. About 20 years ago, researchers started to use microfabrication techniques to study the behavior of cells on micro- and nanopatterned surfaces (Voldman et al, 1999). Since then, many researchers have studied cell-substrate interactions on such designed surfaces using many different materials, designs and cells. In 2001, Chen and Pe'pin used micro- and nanofabrication techniques by using silicon microelectronics methods. In 2006, researchers studied various types of cells reaction to the microtopography (Hasirci and Kenar, 2006; Curtis et al, 2006). Also changes in cell alignment, adhesion, morphology, proliferation, vitality, differentiation and gene expression on different topographies were studied (Martinez et al, 2009). These studies showed that cellular functions can be affected and even enhanced when substrates mimicking the ECM topography were used to grow cells on. This meant that substrates do not just supports the cell growth but also they could guide their adhesion, proliferation, morphology, spreading by providing topographical signals (Martinez et al, 2009). So, in this study an example of this cell-substrate relation will be shown.

## 1.1.1   Substrate Materials

Biomaterials and tissue engineering aim to support, augment or substitute the functions of diseased or damaged organs and tissues. Basic components of human tissues are cells and the extracellular matrix (ECM). Function of the ECM is the provision of a support material, a microenvironment and it also plays an important role in cell metabolic activities and

function. Since ECM has such a great importance for tissues, implant surfaces and scaffolds for tissue engineering applications are designed to mimic the ECM. 3D scaffolds aim to create a similar environment and functionality with that of the ECM. It is comparatively easy to substitute less complex tissues like bone and cartilage but in more complex tissues which have micro- or nanoarchitectures or enhanced vascularization, it is hard to mimic the natural tissue because it needs more specific substrate structures (Gauvin et al, 2012). In order to mimic the ECM of complex structures, it is important to know the functions and properties of it. ECM is composed of the main structural components of the body such as collagen, polysaccharides and elastin (Sell et al, 2010). ECM also has topographical structures like fibers, pores and ridges in nanoscale. These nanostructures can create microscale topographies by folding or bending. Collagens are approximately 300 nm in length and 1.5 nm in width, their fibrils can be as long as tens of microns and have diameters between 260 and 410 nm (Bettinger et al, 2009). Most native ECM has subunit topography. Some examples are papillae of the surface of dermal ECM, osteons in bone tissue, and villi and crypts on the small intestine ECM surface. By using nano- and microfabrication techniques such as photolithography, electrospinning or other various methods, these nano- and microstructures of ECM can be mimicked to some extent. As mentioned above, cells can align or stretch in the direction of these topographies by contact guidance. Contact guidance is the effect of micron and nanoscale structures on the cells of the growing tissues. Contact guidance by the substrate and the surrounding cells has a role in the regulation of migrations that are observed in fibroblast and epithelial cells (Bettinger et al, 2009). Substrate properties like shape, size, geometry, stiffness and elasticity contribute to contact guidance. Cell-ECM interactions have roles in the morphogenesis, pattern formation, phenotype acquisition, wound healing, inflammation, tissue granulation and remodeling (Sell et al, 2010). Cell nucleus-ECM interactions also affect cell adhesion, migration, growth, differentiation, and apoptosis (Sell et al, 2010). Cells can sense the signals originating from the ECM and they respond (Bauer et al, 2009; Huebsch et al, 2010; Levental et al, 2009). ECM component proteins such as collagen, elastin, fibronectin and laminin provide binding sites for cells. Cells can contact these sites through the integrins present on the cell membrane. Through this, the cells can sense the signals coming from the ECM (Hynes, 2009).
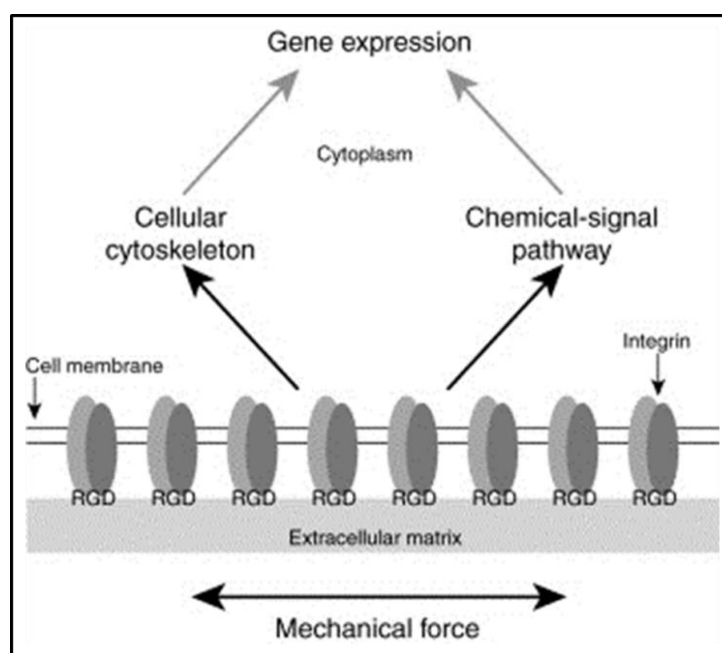
**Figure 1.1** Schematic diagram of cell-susbtrate interactions through adhesion to extracellular matrix (ECM) molecules containing a specific cell-adhesion sequence [Arg–Gly–Asp (RGD)] and subsequent gene expression activation (Kim and Mooney, 1998).

### 1.1.1.1 Synthetic Polymers

Synthetic polymers have some advantages as scaffold materials in tissue engineering applications. They can be fabricated easily to comply with the desired properties of the targeted tissue. Not only the mechanical properties, but also the chemical properties of the synthetic materials can be designed by modification with functional groups by blending or during synthesis. Finally the synthetic polymers like all polymers are mostly biocompatible because they do not include immunological responses and they are not toxic. Some of these polymers are degradable in the body. Examples of these are polyesters such as poly(glycolic acid) (PGA), poly(lactic acid) (PLA) and their copolymers (PLGA), poly(p-dioxanone), and copolymers of trimethylene carbonate (TMC) and glycolide. Polyesters can be easily degraded by hydrolysis of the ester linkages hydrolysis and are used commonly (Gunatillake and Adhikari, 2003). Polyesters such as PLA, PGA and PLGA are also used in bone tissue engineering (Kohn and Langer, 1997; Burg et al 2000). PLGA copolymers are frequently used in bone repair applications (Nelson et al, 1977; Hollinger, 1983). A negative aspect of biodegradable polymers is that their degradation products are acidic and they were shown to decrease the pH significantly.

## 1.1.1.2 Natural Origin Materials

Natural polymers are derived from the nature and have many advantages in tissue engineering applications over the synthetic ones. Since they originate from the nature, they are mostly biocompatible. They might have specific binding sites which can be used to improve interactions during tissue healing and integration. Natural materials also have some disadvantages. They may be immunogenic, denature easily or decompose making it difficult to process them into implants with desired shapes and sizes. Examples of natural materials are collagen, coral, chitin (from insects and crustaceans) and chitosan, keratin (from hair), cellulose (from plants), chondroitin sulfate and hyaluronic acid (Agrawal, 1998).

### 1.1.1.2.1 Collagen

One of the most commonly used natural origin material is collagen. It is a matrix polymer conserved across species. It is the extracellular matrix component of most connective tissues and it constitutes one third of all the protein found in the tissues, especially in the musculoskeletal tissues. It has a great importance in the tissue architecture due to its mechanical properties, too (Cheema et al, 2011). There are at least twenty seven types of collagen known and 80-90% of them in the tissues and the organisms are types I, II and III. Collagen is secreted by fibroblasts and epithelial cells and is triple helix unit (Ha et al, 2013). This triple helix unit is composed of three polypeptide chains with the repeating amino acid sequences Gly-X-Y. In the center of the triple helix is found the Gly residues and the surface is made up of X and Y residues where X is usually proline or hydroxyproline. Hydroxyproline is an important amino acid for the stabilization of the triple helix because it is rigid and hydrophobic and stays on the surface and protect the inside of helix from external compounds (Bou-Gharios and de Crombrugghe, 2008). Most of the collagens are in fibrillar form due to the packing of collagen types I, II, and III. Collagen IV, on the other hand, is a two dimensional structure and unique to the basement membranes. Basement membranes provide physical support for tissues due to their high tensile strength; besides they influence cell proliferation, adhesion, migration and differentiation (Ha et al, 2013). Collagen implants and scaffolds are obtained by extracting collagen from natural tissues. Collagens are highly denatured during the extraction procedure. They are used as scaffolds for tissue replacements and as support matrices (Cheema et al, 2011).
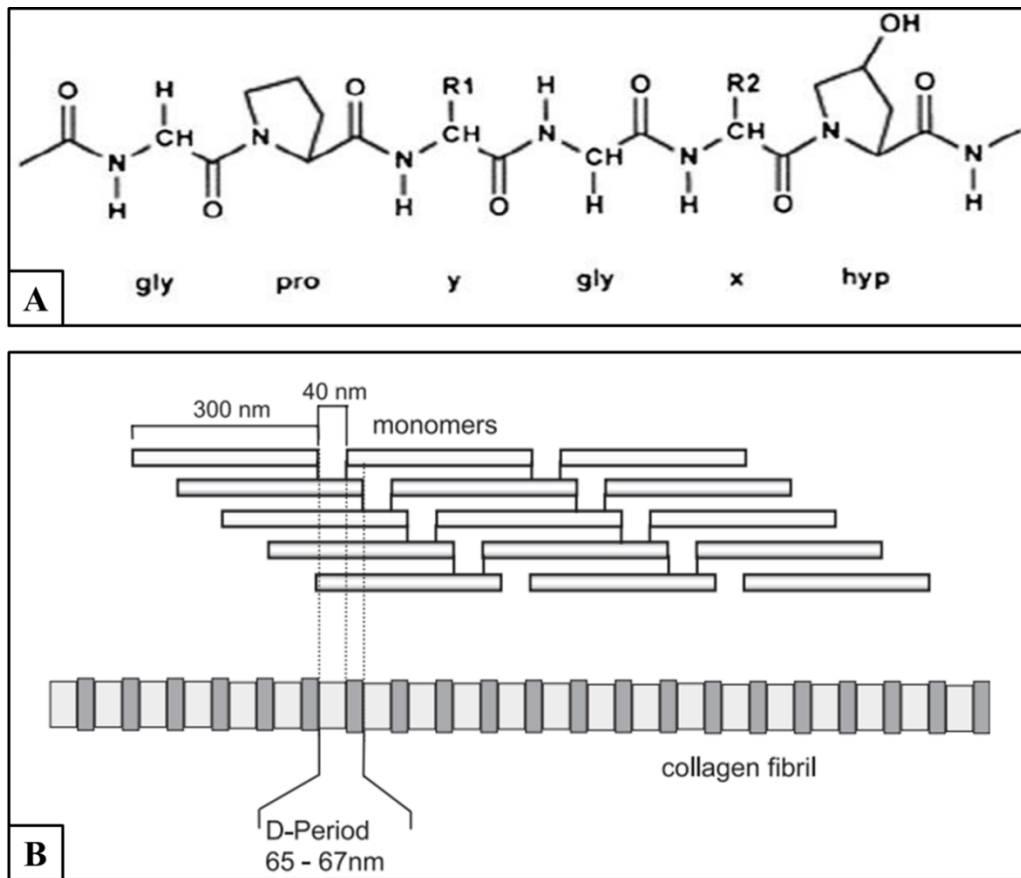
**Figure 1.2** A) Type I collagen structure with Gly residues at every 3<sup>rd</sup> residue. B) Staggered collagen molecules containing 300 nm long and 40 nm gaps separating consecutive monomers providing the structure of the collagen type I fibrils and collagen fibril with 65-67 nm periodicity (Adapted from Gelse et al, 2003; Fullana and Wnek, 2012)

### 1.1.1.2.2 Elastin-like Recombinamer

Recombinant DNA technology is started to be used in material sciences and tissue engineering applications. It involves introduction of a gene to an organism's genetic material, and production of recombinant proteins is possible. These recombinant proteins used in biomaterials studies are called "recombinamers". With this technology, protein based polymers (PBPs) such as elastin-like recombinamers (ELRs) can be produced (Rodríguez-Cabello et al, 2009). ELRs are composed of repeating sequences some of which are found in the mammalian elastic protein, elastin. So ELRs have properties similar to that of elastin. ELRs are highly biocompatible and have self-assembly capability. Most ELRs undergo molecular transition with the change in temperature. A molecular transition of polymer chains (expansion or contraction) occurs above a certain temperature called "Inverse

Temperature Transition" (ITT). Below this temperature, polymer chains are extended and above this temperature, the chains fold and undergo a phase separation and become compact or insoluble (Arias et al, 2006).

ELRs consist of repeating units of the pentapetides Val-Pro-Gly-X-Gly (VPGXG). Here X represents any natural or modified amino acid, except proline or hydroxyproline. ELRs have been used to improve cell attachment on surfaces or in coating products. Some examples of similar sequences are REDV, a recognition sequence for endothelial cell attachment, (VPGIG) a sequence that introduces elastic behavior, and (VGVAPG), target for elastases. These are used in many applications including vascular tissue engineering. The RGD sequence is used to improve cell adhesion in soft tissue engineering applications because it is a sequence found in the natural ECM protein collagen or in fibrinogen (Chilkoti et al, 2006; Rodríguez-Cabello et al, 2009; Kinikoglu et al, 2011).

In this study, the ELR used contained 6 monomers of RGD, a histidine-tag, 6 aspartic acids, 24 lysines and 7 histidines, which are charged residues. This structure is called H-RGD6 (Figure 1.3).
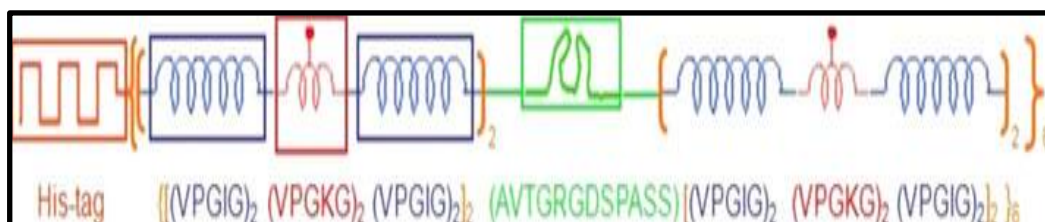


**Figure 1.3** The composition of the elastin-like recombinamer, H-RGD6 used in the present study (Kinikoglu et al, 2011)

It was shown that ELR incorporation decreased the compressive strength and stiffness of the collagen scaffolds possibly due to prevention of collagen crystallization (Kinikoglu et al, 2011).

### 1.1.1.3 Substrate Material Properties

### 1.1.1.3.1        Chemical Properties

Chemical reactions occur immediately after cells adhere to a substrate. First, proteins from the medium are adsorbed onto the surface and cell adhesion occurs. Then the cells release compounds involved in signaling, ECM deposition, cell proliferation and differentiation. These all depend on the chemical interaction of the cell and the substrate, and therefore, the

chemical composition of the surface is among the most important properties affecting the implant performance.

Hydrophobicity, charges and interaction with proteins are all a result of the chemical composition of a substrate material. Studies show that moderately hydrophilic surfaces lead to more cell adhesion and good spreading, proliferation and differentiation on a surface (Goddard and Hotchkiss, 2007; Xu, 2007). In studies with osteoblasts studies, adhesion was found to decrease with increasing contact angle from 0° to 106° and with fibroblast cells, the highest adhesion was observed between 60° and 80° (Tamada and Ikada, 1993; Wei et al, 2009). Protein adsorption is another event occurring just before cell-substrate contact. Many proteins such as immunoglobulins, vitronectin, fibrinogen, and fibronectin adsorb on implant surfaces. After this, inflammatory responses may be initiated (Xu, 2007). Studies show that adsorption of serum albumin before cell seeding prevents fibroblast cells adhesion onto the surface whereas adsorbed fibronectin enhances the adhesion of fibroblasts (Allen et al, 2006).

It has been found that surface charge is another parameter that influences cell behavior on surfaces (Ishikawa et al, 2007). Studies show that positive and negative ions on surfaces can improve their biocompatibility, and the cell affinity to surface and differentiation (Bet et al, 2003). As an example, attachment and spreading of osteoblast and fibroblast were shown to be improved more with the positive charges surfaces compared to negative and neutral (Schneider et al, 2004). In one study, polyethylene surfaces were modified to carry different charged groups (-COOH, -$CH_2OH$, -$CONH_2$ and –$CH_2NH_2$ groups) and cell behavior was studied. Results showed that cells adhere more when charged functional groups are grafted on surfaces. Also there were differences in cell spreading with differences in surface groups. For example, chinese hamster ovary (CHO) cells spread more on surfaces with hydroxyl groups than surfaces with neutral functional groups and it was thought that hydrogen bonds between the surface hydroxyl groups of the polymer and cell surfaces polar groups caused this higher spreading (Lee et al, 1994). Keselowsky et al (2005) showed that hydroxyl and amine groups can improve osteoblast-specific gene expression, alkaline phosphatase enzymatic activity, and matrix mineralization when compared to carboxyl and alkyl groups.


### 1.1.1.3.2    Physical Properties


Microscale structure of tissue engineering scaffolds has a great impact on cell behavior. For example, cell behavior on surfaces with edges, grooves or pillars is different than on smooth surfaces. In many studies, cells show orientation or migration along the fibers or ridges on the surfaces of the substrates. Fibroblasts were shown to orient on grooves (or channels) when the widths are between 1 and 8 μm and the degree of this orientation depends also on the depth of the grooves. Each cell type needs different surface topography for optimal adhesion, migration and proliferation (Dunn and Brown, 1986). Materials crystallinity, porosity, pore size, pore interconnectivity and tortuosity are all important factors (Hutmacher, 2001). Scaffold porosity has a role in nutrient provision, cell signaling, and waste disposal. So, physical properties of the pores are very important for cell-cell interaction and cell growing on substrates (Karageorgiou and Kaplan, 2005).

### 1.1.1.3.3    Mechanical Properties

Mechanical properties of a substrate material is very important parameter affecting the cell behavior on the scaffolds. Balance between scaffold mechanical properties and architecture is also important for cell infiltration into cell carriers and for vascularization of the carrier (O'Brien, 2011). Surface roughness and stiffness are the main parameters that affect the response of cells to substrates.

In a study, it was shown that ALP activity, proliferation and expression of calvarial osteoblastic cells were higher on rough surfaces with average roughness up to 0.8 μm compared to the smooth ones (Hatano et al, 1999). Human osteoblastic cells were also shown to have increased spreading and proliferation on rough surfaces (Lim et al, 2005). Surface roughness can be macro- (100 μm – milimeters), micro- (100 nm – 100 μm) or nanolevel (less than 100 nm). Cells respond differently depending on the roughness level (Agaska et al, 2010). Also different cell types give different responses to roughness. Surface roughness can be considered for the cells large enough such as osteoblast and neuron (Donoso et al, 2007). All these indicate that surface roughness should be considered in cell-surface interaction according to the cell type. Also there are several studies on stiffness. For example, when mesenchymal stem cells were grown on rigid gels, differentiation through muscle forming was observed due to the elasticity of the gel similar to the muscle and when the neural stem cells were seeded on soft scaffolds having similar mechanical property with normal brain tissue, neuron differentiation was observed (O'Brien, 2011).

### 1.1.1.3.4    Shape of the Physical and Chemical Patterns

Shape of the nano and micropatterns is another parameter that affects the cell behavior. It was found that when a fibronectin coated disc shape with 700 μm² size and 100μm gaps is used, human MCF10A mammary epithelial cells are polarized randomly and divide in any direction and cells on the discs had round shapes. (Tseng et al, 2011). When a fibronectin coated surface with crossbow shape (700 μm² size and 100μm gaps) is used, RPE1 cells (retinal pigment epithelial human cell line) were strongly polarized. Actins and lamellipodia of the cells are at the upper edges of the pillars whereas the acto-myosin contraction took place at the bottom edge of the crossbow shape. Also, HeLa cells, human adenocarcinoma epithelial cell line, on fibronectin coated micropatterns can orient their mitotic spindle relative to the pattern geometry (Thery et al, 2006 a; Thery et al, 2007). When a fibronectin coated H shaped pattern (700 μm² size and 100μm gaps) was used with HeLa cells, actins and lamellipodia were placed at the edges. Mitotic spindles are oriented along the vertical axis. Also the cells are symmetrically oriented by division (Thery et al, 2005; Thery et al, 2006 b). Fibronectin coated Y shaped patterns (700 μm² size and 100μm gaps) are also used and HeLa cells show triangular shape with their actin and lamellipodia on these patterns. Finally, when fibronectin L shaped patterns (700 μm² size and 100μm gaps) are used, HeLa cells also show triangular shape with their actin and lamellipodia on these patterns (Thery et al, 2006 b).

Disc shape    Crossbow shape    H shape    Y shape    L shape
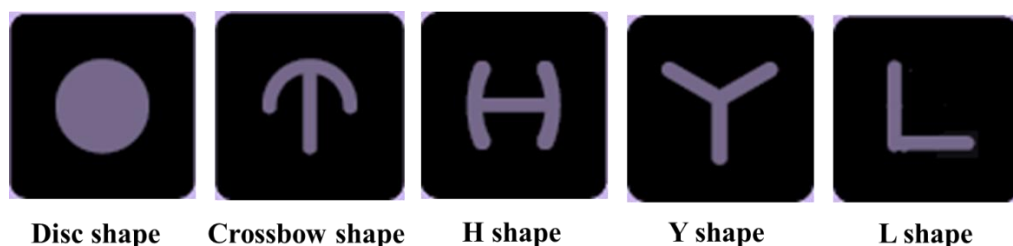
**Figure 1.4** Schematic representations of micropattern shapes (Adapted from Cytoo, 2013)

### 1.1.2    Micro and Nanostructure Fabrication and Substrate Production Methods

Micro and nanofabrication means production of micro and nanoscale structures using a variety of techniques. Cells are cultured on such substrates. Fabrication methods can be divided into two categories as bottom up and top down. Top down techniques used are photolithography, microcontact printing, microtransfer molding, capillary force lithography, and scanning probe lithography (SPL). Selfassembly and rapid prototyping can be considered as a bottom up technique (Coutinho et al, 2011).

#### 1.1.2.1 Photolithography

Photolithography is formation or removal of a polymer network on a substrate by using UV exposure of a photo mask coated with a resin. The substrate is a silicon wafer and the photo mask is a semitransparent film that allows UV passing through (Berkowski et al, 2009). Highly intense UV is used to transfer the pattern on the template or mask to the surface of substrate (Subramani, 2009; Berkowski et al, 2009). Photomasks are generally transparent glass plates and patterns (or their inverse) are mostly metals that block UV transmission (Nguyen, 2008).

In the photolithography process, there are 4 basic steps: positioning of the mask on the substrate, exposure with UV, and development of the resin and finally etching of the silicon layer. The positive resists used in coating the substrate become more soluble in developer solution after UV exposure while the negative resists become polymerized or crosslinked and become more difficult to dissolve after exposure. In the development step, the soluble parts of the resist are dissolved (Nguyen, 2008). Photolithography technique when applied to thick resists the resultant resist can also be used in fabrication of thick tiny reactors for making micro channels (Nguyen, 2008).

### 1.1.2.2 Soft Lithography and Microcontact Printing

Micro and nanostructures can be constructed with soft lithography technique by using polymers such as polydimethylsiloxane, PDMS as templates or stamps. A typical example is microcontact printing which basically is a method similar to using a regular stamp or ink. Soft lithography has the advantages of low cost and ease, and is frequently used in cell micropatterning. Also curved surfaces can be used easily due to elasticity of PDMS while photolithography is not suitable for such surfaces (Wen-Wen et al, 2009).

Microcontact printing is another technique used to pattern molecules on a surface for cell behavior and protein adsorption applications. In microcontact printing, PDMS is used to produce a stamp by replica molding. Then the stamp is inked to adsorb cells, proteins and other molecules in order to transfer them to the substrate. After the stamp is pressed, the solvent is evaporated and printed molecules are transferred, stamp is removed and the patterns are revealed. Microcontact printing can be used for large areas, and multiple copies of the patterns can be obtained by a single stamp applying it repeatedly. These are some advantages of the technique. However, it has some disadvantages such as the amount of material adsorbed on the stamp is not easy to control and the stamp may swell leading changes in the pattern geometry. Contamination can be a problem due to unpolymerized siloxane of stamp (Coutinho et al, 2011). Production of patterns with some height (3D patterns) is not possible with this technique.

### 1.1.2.3 Electron Beam Lithography

Electron beam lithography (EBL) has the capability to produce very small patterns with dimensions up to 3-5 nm. It needs an electron source and a scanning electron microscope to perform its design transfer. Electrons from this electron source are accelerated in an electron field, where the electron beam is focused to a narrow spot which is 2-5 nm by passing the lenses. EBL is a process similar to photolithography; photolithography can expose a whole wafer at once but EBL makes it in a serial, so it takes a long time. In addition, the stage movement, calibration and settle time are slow and long. Fabrication procedures of EBL and photolithography are also similar in that both use a resist to coat the substrate. However, EBL uses an electron sensitive polymer coat instead of a light sensitive one. This polymer either breaks down or crosslinks during exposure. Then in the development step, exposed patterns are revealed. In the EBL process, conducting substrates or metallic films coated non-conducting substrates are used (McMurray et al, 2011).

### 1.1.2.4 Hot embossing

Hot embossing is another technique widely used for micropatterning. Thermoplastic polymers are used in this technique and heat is applied to polymer above its transition temperature until the polymer softens. Then the master is pressed onto it and cooled down.

When cool the master is released from the polymer replica. It is a very simple and short procedure (McMurray et al, 2011).

### 1.1.2.5 Self-assembly

Molecular self-assembly technique gets its origin from the natural world such as oil drops fusing in water, or tetrameric hemoglobin protein formation from four hemoglobin subunits. Self-assembly uses noncovalent, weak bonds such as hydrogen bonds, hydrophobic interactions and van der Waals or ionic interactions. For synthetic material self-assembly procedures, peptides and proteins are used as templates (Zhang, 2003). Micro and nanofabrication through selfassembly has the advantage of producing nanoscale designs, does not lead to size differences due to the shrinking of the patterns on nanoscale and it can produce 3D structures. There are two approaches in this technique: One, molecules interact with each other using hydrogen bonds, ionic bonds, hydrophobic interactions and van der Waals. Two, external forces (eg. electrostatic, magnetic, hydrodynamic) are used to obtain the desired organization (Parviz et al, 2003).

### 1.1.2.6 Rapid Prototyping

Rapid prototyping (RP) is a more recent technique that benefits from the computer technology and is a bottom up process. It can reproduce complex products quite rapidly with information received directly from a computer model or a system like CT (Yang et al, 2002). RP uses additive processes. Its components are built up gradually in layers until the final geometry is obtained (Upcraft and Fletcher, 2003). Rapid prototyping technique can produce scaffolds for cell seeding and cell encapsulation and design 3-dimensional microstructures with predetermined architecture (Billiet et al, 2012). An important property of RP is the ability to build predefined macrostructures as well as microstructures such as objects within objects which are not possible with the traditional fabrication methods. This property makes RP a very useful technique for fabricating scaffolds with controlled structures and architectures for use in tissue engineering and also in implant preparation (Yang et al, 2002). The materials that can be used to construct parts with RP are polymers (natural or synthetic) and metals. Ceramics can be used in the forms of blends. RP can be used to reconstruct parts of the body such as bone fragments. For example, an ear or a jaw can be constructed to fit the contours of the organ of the patient obtained directly from the patient by magnetic resonance imaging (MRI) or CT scan (Yang et al, 2002). There are several different RP approaches and all of them follow the same basic five steps: (i) Creation of the CAD model of the design or the targeted tissue, (ii) Conversion of the CAD model to STL (Standard Tessellation Language) format, (iii) Slicing of the STL file into thin cross-sectional layers, (iv) Layer by layer construction, (v) Cleaning and finishing (Patra, 2010). Each RP technique has its own advantages and disadvantages (Upcraft and Fletcher, 2003). Resolution, materials, and fabrication techniques are unique to each RP method but all are economical and time efficient for modifying and fabricating 3D devices (Tek et al, 2008).

### 1.1.3    Responses of Cells and Their Nuclei to Patterned Substrates

### 1.1.3.1 Anatomy of Cell and Nuclei

All mammalian cells have a plasma membrane which is basically a lipid bilayer containing some proteins and polysaccharides. The membrane functions as a barrier and controls the transfer of the molecules between the inside and outside of the cell. One role of the membrane proteins is to link the membrane to the cytoskeleton, ECM, or other cells (Luna and Hitt, 1992; Yamada and Miyamato, 1995; Maniotis et al, 1997). Interior of a cell is the cytoplasm which carries in it the organelles and a nucleus.
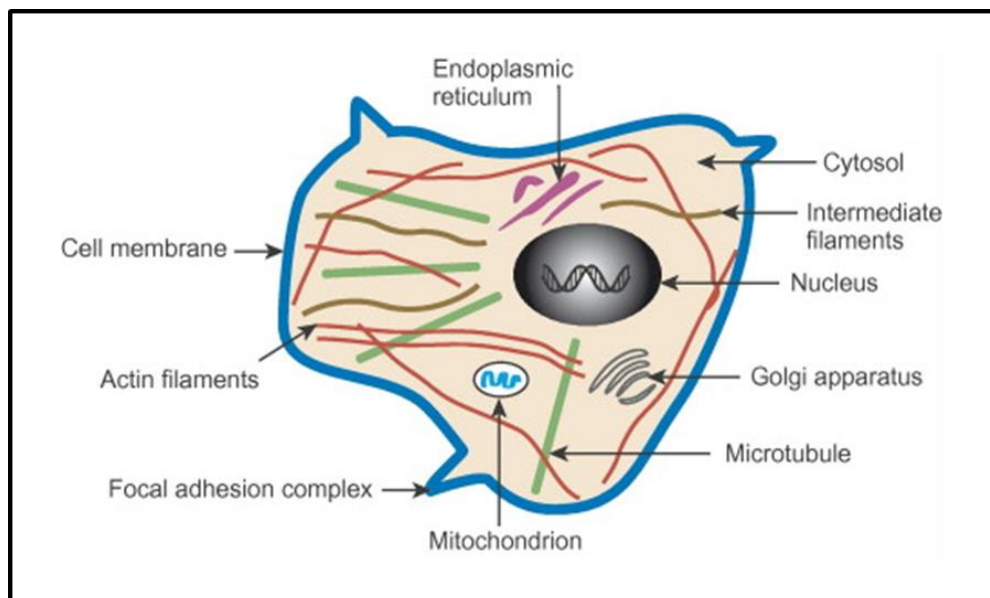


**Figure 1.5** Schematic representation of cell structure (Suresh, 2007)

Cytoskeleton of a cell is a large protein filament network (Maniotis et al, 1997; Janmey, 1998). Cytoskeleton also defines the cell shape and contributes to its resistance to deformation and elasticity for processes such as transportation inside the cell or cell division and mobility (Elson, 1998). Cytoskeleton consists of: (i) microfilaments (composed of actin), (ii) microtubules (composed of tubulin), and (iii) intermediate filaments (composed of fibrous proteins like vimentin and lamin). Filaments are also the components of the microspikes, the protrusions of plasma membrane, and the lamellipodia, the extensions from the cell surface. Actin filaments are both very resistant to deformation but still they are flexible enough (Janmey et al, 1991). Microtubules play a role in the localization of membrane bound organelles and the components inside the cell, and they are also stabilizing

elements (Janmey et al, 1991; Alberts et al, 1994). Intermediate filaments are around the nucleus and they extend from the cytoplasm and reach to cell membrane (Goldman et al, 1996). They are mostly found in cells subjected to mechanical stress and they maintain the shape and give mechanical properties of the cell (Goldman et al, 1998).
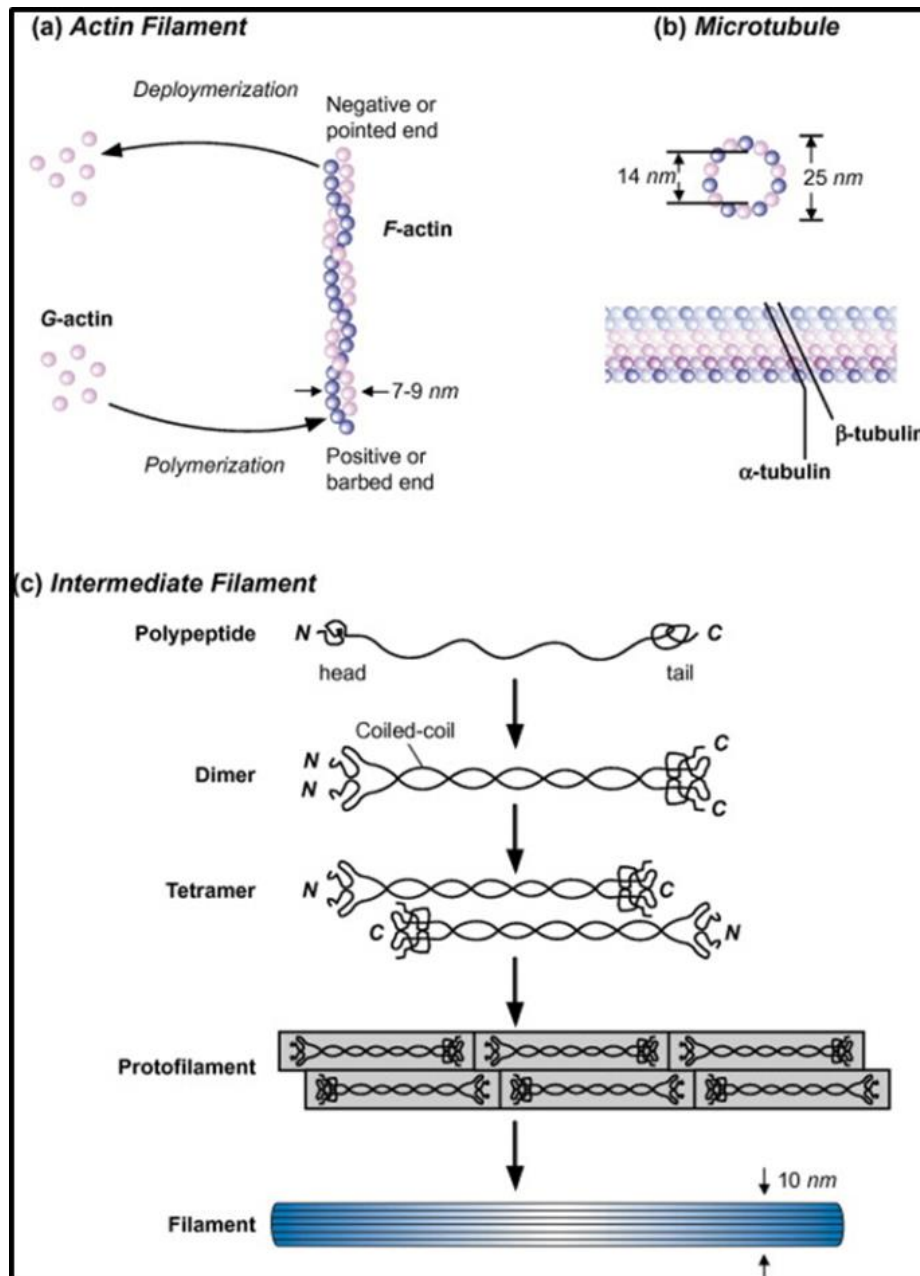


**Figure 1.6** Schematic representations of three structures of cytoskeleton (Suresh, 2007)

Major component of the cell is the nucleus. All nuclei of mammalian cells have a nuclear envelope, nucleoplasm, nuclear lamin and nuclear pore complex (Stuurman et al, 1998). The nucleus carries the genetic information of the cell in the chromosomes. Every cell in a body has the same genes. It was reported that nucleus is stiffer than the cytoplasm of the cell (Guilak et al, 2000; Caille et al, 2002). Even the nucleus interacts with the cytoskeleton, it has its own mechanical strength and it is thought that the one of the components that contributes to this stability is the lamina. Lamina is a crosslinked protein and it interacts with the inner nuclear membrane proteins. Shape of the nucleus is a result of this structure. Lamina is composed of lamins (lamins A and B). The A-type plays a role in differentiation and the B-type in viability of the cells (Rowat et al, 2008).
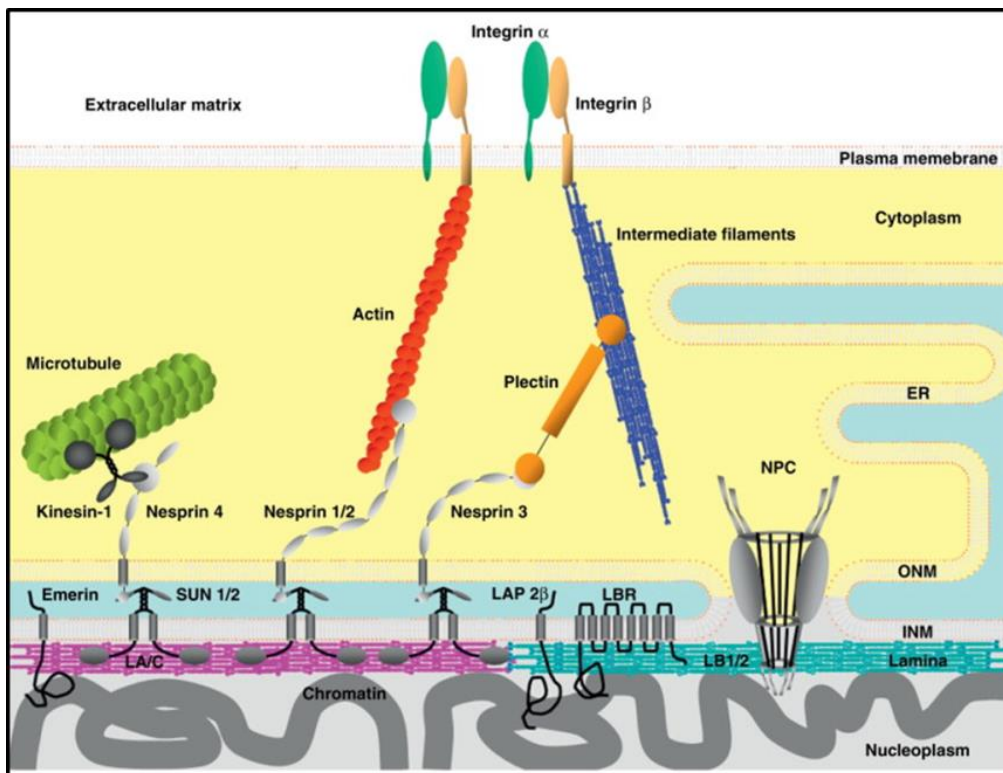


**Figure 1.7** Schematic representation of interconnectiviy between nuclear envelope and cytoskeletal elements (Shimi et al, 2012)

### 1.1.3.2 Biomechanics of Cells and Nuclei

There are studies showing the biomechanical regulations and pathways in cell and nucleus. For example, nucleus deformation mediated by the cytoskeleton may be caused by a shear

stress leading to a gene regulatory signal. Also stiffness of the nuclear envelope can influence the force acting on chromatin. These studies show that nucleus biomechanics of nuclear deformation induced by force is very important (Deguchi et al, 2005). While studying the nucleus and the biomechanics of deformation, three structures should be carefully considered: (i) the lipid bilayer, (ii) nuclear lamin, and (iii) the nucleoplasm. In a study of Guilak et al (2000), deformation of isolated nucleus was studied by using micropipette aspiration. The results show that in the isolated cells, the mechanical contribution of the nuclear envelope stiffness is more important than nucleoplasm (Guilak et al, 2000). Many studies were conducted on nucleus biomechanics and most of them showed the importance of differences in the stiffnesses of the nucleus and the cytoskeleton because mechanical forces are transmitted to the nucleus by the cytoskeleton. Methods like micropipette aspiration showed that nuclei of chondrocyte, neutrophil and endothelial cells are all stiffer than the cytoplasm (Guilak et al, 2000; Dong et al, 1991; Caille et al, 2002). In addition, cells have the ability to adapt their shape and cytoskeleton to the substrate material stiffness (Yeung et al, 2005). Also it was observed with chondrocyte, neutrophil and endothelial cells that their nuclei deformation was less than that of the rest of the cell (Hoffmann et al, 2007). For attached cells, mechanical stimuli from the ECM are transferred directly from the cell membrane to the nucleus. During cell attachment, spreading and migration, a certain mechanical energy is produced. The forces on the cells and the resulting cellular deformations cause several processes such as changes in morphology, growth, differentiation, gene expression and in ECM (Vandenburgh, 1992; Clarke and Feeback, 1996; Frenette and Tidball, 1998; Mol et al, 2003). Cells may undergo changes to adapt to these stimuli or they are damaged or die if they cannot adapt (Zhu et al, 2000).
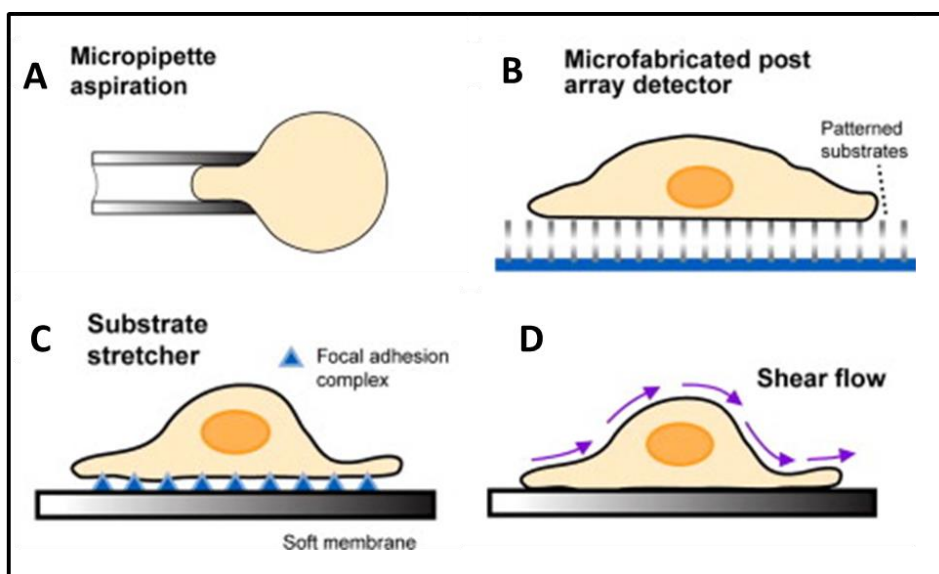


**Figure 1.8** Schematic representation of forces applied on cell. A, B) Biophysical forces applied for deformation of single cell, C, D) Techniques used for adhesion, mobility and deformation of cells (Suresh, 2007)

**1.1.3.2.1     Biomechanics of Saos-2 Human Osteosarcoma Cell**

Osteosarcoma is the most common sarcoma and is seen in children and adolescents. Saos-2 is a cell line which was isolated from an 11-year old Caucasian female in 1975. Characteristic properties of this sarcoma are abnormalities in cell proliferation and function (Benayahu et al, 2002). All osteosarcoma cell lines including Saos-2 have a 2 to 3-fold greater doubling time than osteoblasts. Saos-2 cells express the osteoblastic markers such as osteocalcin, bone sialoprotein, decorin and procollagen-I (Pautke et al, 2004). Osteoblasts produce a complex of ECM proteins called the osteoid and these are normally mineralized. However, in osteosarcoma, there is an extensive but incomplete mineralized matrix production (Benayahu et al, 2002). Osteoblastic properties of human osteosarcoma cell line, SaOs-2, were studied and it was found that they have a high ALP activity level (Rodan et al, 1987). This ALP activity was similar to that of human primary osteoblast cells for early time points whereas the activity jumps to 120-fold higher level after 14 days of seeding (Saldana et al, 2011). The collagen they produced is similar to that of primary human osteoblast cells but this collagen has a higher level of lysyl hydroxylation (Fernandes et al, 2007). Finally, expression of cytokine and growth factors of SaOs-2 cells is similar to primary human osteoblast cells (Bilbe et al, 1996).

**1.1.3.3  Cell- Substrate Interactions and Responses**

Substrate topographies can affect the cells at different levels due to the differences in cell type, pattern size and geometry, physical or chemical properties of the substrate material, and stiffness of the substrate material (Bettinger et al, 2009). Surface topography of a substrate can change the cell shape, rate of migration, adhesion and proliferation. Sub-micron to nanoscale topographies affect at cellular level since they have similar size range with ECM proteins such as fibronectin, collagen or laminin fibers. Sub-millimeter scale affects the activity of the tissue subunits such as intestinal villus, bone osteons or dermal papillae. These tissue subunits contain a large number of cells so, sub-millimeter topography can also affect cell-cell interactions, cell-cell signaling, and other cellular activities (Wang and Carrier, 2011). In the present study, microscale topographies were studied and their effect on cell adhesion, proliferation, mobility, differentiation and conformational change were determined.

**1.1.3.3.1     Adhesion**

For cell growth on a surface, the first requirement is the attachment of the cell to the surface. Cell adhesion can also affect their spreading, migration and differentiation. There are many studies and techniques developed to quantify the extent and strength of cell adhesion. Commonly used approach involves suspension of cells on the surface, incubation in culture medium, and removal of weakly adhered cells (Lauffenburger and Linderman, 1993). It is

very difficult to generalize the cell adhesion behavior for various cell types on micro and nanostructures. For example fibroblast cell adhesion was shown to decrease on nanopatterned surfaces whereas muscle cell and astrocyte cell adhesion was increased. Another study reported that peptide covered nanodot ($\leq 8$ nm) patterned surfaces with 58 nm spacing were suitable for cell adhesion whereas 73 nm spacing were not and MC3T3 cells (osteoblast precursor cell line) could not adhere (Martinez et al, 2009). In order to find the optimal physical cue sizes, one approach could be to use sizes similar to the ECM protein dimensions and this may increase cell adhesion. Finally, it was found that patterns in grating shapes enhance adhesion whereas nanoposts and nanopits seem to reduce initial cell attachment when various cell types and substrate materials in various dimensions were studied (Bettinger et al, 2009).
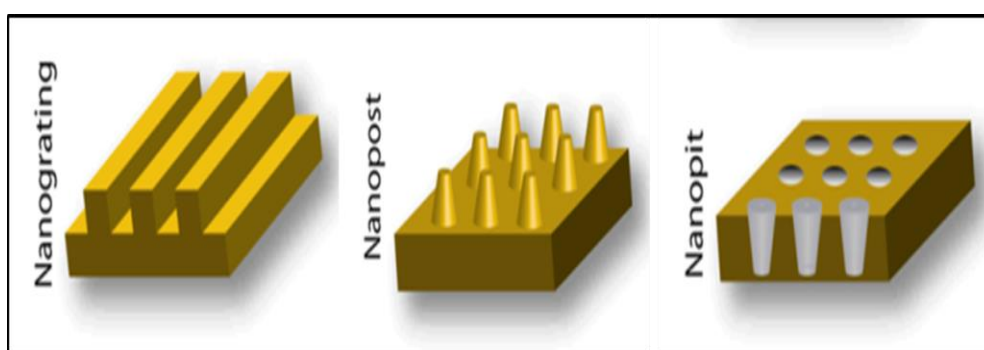


**Figure 1.9** Schematic presentations of nanopatterns (Santos et al, 2011)

### 1.1.3.3.2    Proliferation

Proliferation is another cell property that is affected by substrate topography. In a study it was shown that nanogratings reduced cell proliferation when compared with planar substrates (Bettinger et al, 2009). However, in general, it is hard to predict the proliferation behavior of the cell on patterned substrates (Bettinger et al, 2009). In another study, it was said that effect of nano and micropatterns on cell proliferation depended on the cell type (Green et al, 1994; Dalby et al, 2004; Miller et al 2004). In literature, studies focus generally on the microscopic images of cells instead of quantification of proliferation, and this may be the reason for the insufficient information about cell proliferation upon interaction with patterned substrates. In general, researchers prefer proliferative cell lines such as fibroblasts, osteoblasts, carcinoma lines to study this phenomenon, and this may the cause of the limited and biased results. Also another study showing the effect of topography on proliferation was on human embryonic stem cells. These cells show a reduction in proliferation on nanopatterned substrates (Gerecht et al, 2007). In the literature, a few studies on cell

proliferation-substrate interaction show a decrease in cell number on the substrate but there are also some studies that report an increase in cell proliferation on patterned substrates (Popat et al, 2007).

### 1.1.3.3.3 Differentiation

There are a few studies on cell-substrate interactions affecting the cell differentiation in the literature. These studies show that nanostructures cause differentiation of mesenchymal stem cells into osteoblasts without any promoter for osteogenic differentiation in the culture medium (Dalby et al, 2006; Dalby et al, 2007). Another study reported an increase in ALP of marrow stromal cells on nanoporous alumina substrates when compared to amorphous alumina surfaces with no nanoarchitecture (Popat et al, 2007). ALP activity was observed in human mesenchymal stem cells (hMSCs) after 2 weeks of culture on micropost arrays with diameter of about 2 μm, heights of 1–12 μm and spacing of 4 μm between the microposts. Also on the 7th day of the culture, hMSCs on microposts showed osteogenic differentiation (ALP activity) possibly due to microposts (Fu et al, 2010). Finally, it was shown that human mesenchymal stem cells differentiated preferentially into neuronal linages on bovine collagen I coated PDMS nanograting and nanopit (350 nm in depth, 350 nm width and 700 nm pitch) patterned surfaces (Yim et al, 2007). All these results indicate that topography can direct cell fate.

### 1.1.3.3.4 Mobility

Cell motility is another property affected by cell-patterned surface interactions. There are reports of several cell types such as endothelial cells (Bettinger et al, 2008), epithelial cells (Dalton et al, 2001; Rajnicek et al, 2007), osteoblasts (Lenhert et al, 2005) and C6 glioma cells (Wang et al, 2008) migrated in the direction of grating patterns. These cells also showed an increase in the migration velocities on these surfaces. In addition, it was observed that migration of these cells was directed by topography and proof of this was the polarization of microtubule organization centers of the cells (Yim et al, 2005). In many studies, it was also observed that migration is coupled with the elongation of the cell and alignment of the cell body with nanopatterned surfaces (Lenhert et al, 2005; Bettinger et al, 2008; Wang et al, 2008). Lastly, in a study, nanoposts were observed to cause biased and increased velocity of migration of the cell (Tzvetkova-Chevolleau et al, 2008).

### 1.1.3.3.5 Conformational Change

In the literature, the most obvious effect of topography was observed on cell morphology. Many cell types such as fibroblasts, endothelial cells, stem cells, smooth muscle cells, epithelial cells and Schwann cells have presented conformational changes on patterned surfaces (Hsu et al, 2005). Conformational responses were seen with the pattern sizes as low

as 100 nm and depth around 75 nm (Loesberg et al, 2007). Most responses were amplified with decreasing pitch and increasing depth. Several studies showed filopodia formation (Hart et al, 2007) and decrease in adhesion complex formation (Biggs et al, 2007). Morphological changes were not always observed with all types of cells. In many studies, grooves caused elongation and polarization in nuclear structures for all sorts of cells (Wojciak-Stothard et al, 1995). Another study with polystyrene groove patterned surfaces shows that in the largest grooves (0.5 μm depth and 10 μm width), RBM (Rat bone marrow) cell membranes conform to the grooves whereas in narrowest and deepest grooves (1.5 μm depth and 1 μm width) cells made bridges on the grooves with their extensions (Matsuzaka et al, 2003). Lastly, wells, pits and pillars with dimensions less than 5 mm showed smaller and round shaped cells and less organized cytoskeleton for a number of cell types (Hunt et al, 1995; Gallagher et al, 2002; Dalby et al, 2002; Andersson et al, 2003). Also another study indicates that the deformations were due to mechanical deformation causing bulk mass of the nucleus to be placed in between the pillars (Davidson et al, 2009). These cells are adherent cells and need large surfaces to spread on and make contact needed for mobility, cell division and other activities. When the top surfaces of the pillars are sufficiently large (comparable to that of the cell) and more importantly the gaps in between are too narrow for the cells to fit in, they stay on top. Otherwise they slip between the pillars, take contorted conformations. If the gaps were much larger, the cells would have been less contorted or more flat and spread (Davidson et al, 2009).

## 1.1.4 Aim and Novelty of the Study

Interaction between cells and substrates are important because many studies show that there is a strong relation between them. So, this topic has been studied by many researchers recently and, 2D and 3D substrates with micro- and nanotopographies were started to be used in tissue engineering (Dalby et al, 2002; Curtis et al, 2006; Hasirci and Kenar, 2006; Davidson et al, 2009; Lin et al, 2013). The aim of this study is to observe this effect of pattern dimension and spacing on the cell-material interactions on cell attachment and cell and nuclei conformational change. The use of an ELP-Collagen blend was expected to also influence this interaction. The selection of the pattern dimensions was such that they could lead to nuclear morphology changes and to study the relation between nucleus bending and proliferation rate was expected to provide a better understanding.

# CHAPTER 2

# MATERIALS AND METHODS

## 2.1 Materials

Silicon wafers with the design involving 4 regions covered with 8x8 µm² and 16x16 µm² pillars separated by either 4 or 8 µm gaps with a height of 5 µ were produced by Dr. Umut Atakan Gurkan with MEMS technology at Prof. Utkan Demirci's Bio-Acoustic MEMS in Medicine Laboratory, at Harvard-MIT Health Science Institute, (Cambridge, MA, USA).

Elastin like recombinamers (ELRs) called H-RGD6 in this study containing 6 monomers of RGD, a histidine-tag, 6 aspartic acids, 24 lysines and 7 histidines, which are charged residues, were synthesized in the laboratory of Prof. Dr. J. Carlos Rodriguez Cabello, University of Valladolid (Spain).

Sylgard 184 Silicone PDMS polymer and Sylgard 184 Curing agent were bought from Dow Corning Company (UK).

Bovine serum albumin (BSA), sodium azide (ReagentPlus®, ≥99.5%), sodium cacodylate (pH 7.4), glutaraldehyde (25%), 4',6-diamine-2-phenylindole dihydrochloride (DAPI), FITC-conjugated phalloidin, Amphotericin B, Paraformaldehyde, Penicillin/Streptomycin were purchased from Sigma-Aldrich (USA).

RPMI 1640 cell culture medium, Fetal bovine serum (FBS), SnakeSkin pleated dialysis tubing and Trypsin (0.25%) were obtained from HyClone, Thermo Scientific (USA).

Triton X-100 was purchased from AppliChem (USA).

Trypan blue (0.4 %), goat serum, Alexa Fluor 488 goat anti-mouse IgG, and Alexa Fluor 532 Phalloidin were purchased from Invitrogen (USA).

Primary antibodies for Lamin A (Mouse monoclonal [133A2]) to Lamin A were bought from Abcam plc (UK).

Vancomycin hydrochloride was obtained from Hospira (UK)

Sprague-Dawley rat tails to extract collagen type I from were kindly provided by Dr. Tayfun İde of GATA Animal Experiments Laboratory (Turkey).

## 2.2 Methods

### 2.2.1   Collagen Type 1 Isolation

Collagen Type I was isolated from rat tails as described previously (Franke et al, 2000; Ber et al, 2005; Zorlutuna et al, 2009). Tail skins of the Sprague-Dawley rats were dissected by making a full incision and the tendons were removed. Dissected tendons were then dissolved

in 0.5 M cold acetic acid solution at +4 °C. Then the solution was filtered through glass wool dialysed against dialysis buffer (5 L, 12.5 mM sodium phosphate dibasic, 11.5 mM sodium phosphate monobasic, pH 7.2), for five days in a dialysis tubing (10,000 CO). Dialysis buffer was changed daily. The precipitated collagen was centrifuged at 1,600 g for 10 min (Sigma 3K30, Germany) at +4 °C, the pellet was dissolved in 0.15 M acetic acid. The collagen was precipitated in NaCl solution (5% w/v), centrifuged step was applied (10 min, 16,000 $g$), and the pellet was dialyzed again after dissolving in 0.15 M acetic acid. Collagen precipitate in the dialysis tubing was recovered with centrifugation, and the pellet was stored in 70% ethanol while stirring for 2 days. Finally, the precipitate was centrifuged, and the pellet was lyophilized after freezing at -80 °C (FreeZone 6, Labconco Co., USA) for 12 h. The dry collagen was kept at 4 °C for long term storage.

### 2.2.1.1 Characterization of the Collagen

Characterization of the collagen isolated from the rat tails by SDS-PAGE. For separating gel, 12% (w/v) acrylamide:bisacrylamide (37.5:1, w/w) and for stacking gel, 4% (w/v) acrylamide:bisacrylamide (37.5:1 w/w) were used. Collagens (0.2% w/v collagen in 0.05 M acetic acid) were denatured at 95 $^{o}$C for 5 min. For staining, 0.2% (w/v) solution of Coomasie Brillant Blue (12:50:38 HAc:MeOH:$H_2O$) and for destaining (10:50:40 HAc:MeOH:$H_2O$) were used. Electrophoresis system was set at 30 mA for 2.5 h (Bio-Rad Power Pac HC, Finland).

### 2.2.2 Elastin-like Recombinamer (ELR) Isolation

For films prepared from ELR-Collagen, elastin-like recombinamer (ELR) was used. It was produced and isolated from Escherichia coli (*E. coli*) and characterized. All these steps were carried at the University of Valladolid (Spain). The ELR used in this study contains 6 monomers of RGD, a histidine-tag, 6 aspartic acids, 24 lysines and 7 histidines charged residues and it is named as H-RGD6 as shown in the Figure 1.1 (Arias et al, 2006).

### 2.2.3 Preparation of Micropatterned Silicon Wafers

Micropillar covered master wafers were fabricated at Harvard University, Center for Nanoscale Systems (Harvard CNS, Cambridge, MA) by Umut Atakan Gurkan, Ph.D. Micropillar geometries and dimensions determined at METU BIOMAT were implemented using LayoutEditor Software (EAGLE PCB, USA) as follows: The design involved 4 regions covered with 8x8 μm² and 16x16 μm² pillars separated by either 4 or 8 μm gaps with a height of 5 μ (Figure 2.1). The design was printed on a 10x10 cm glass mask using a Heidelberg mask writer (DWL-66, Heidelberg Instruments, Germany) with submicron level resolution. 100 mm diameter round silicon wafers (University Wafers, USA) were used. The silicon wafers were first cleaned using a combination of methanol, ethanol and isopropyl

alcohol, followed by complete drying for 10 minutes at 210 °C on a hot plate. Then, the wafer was cooled and spincoated using a Headway Spin Coater (PWM32, Headway Research Inc., USA) with OmniCoat (MicroChem, USA) according to manufacturer's instructions to improve SU8 adhesion. SU8 2010 was then spin coated on the wafer according to manufacturer's recommendations. Then, a mask aligner (SUSS MJB4 Mask Aligner) was used to precisely locate the mask on the wafer with undeveloped SU8 coating. A 100 mW/cm$^2$ UV source was used to expose the coated wafer in the mask aligner. After exposure, SU8 developer was used to remove the non-exposed SU8 regions on the wafer. Then, the wafer was washed with isopropyl alcohol and dried at room temperature. Finally, the wafer surface with micropillars was silanized (with aminopropyltriethoxysilate) for 24 h in a vacuum chamber to minimize PDMS adhesion and to enable easy peel-off.
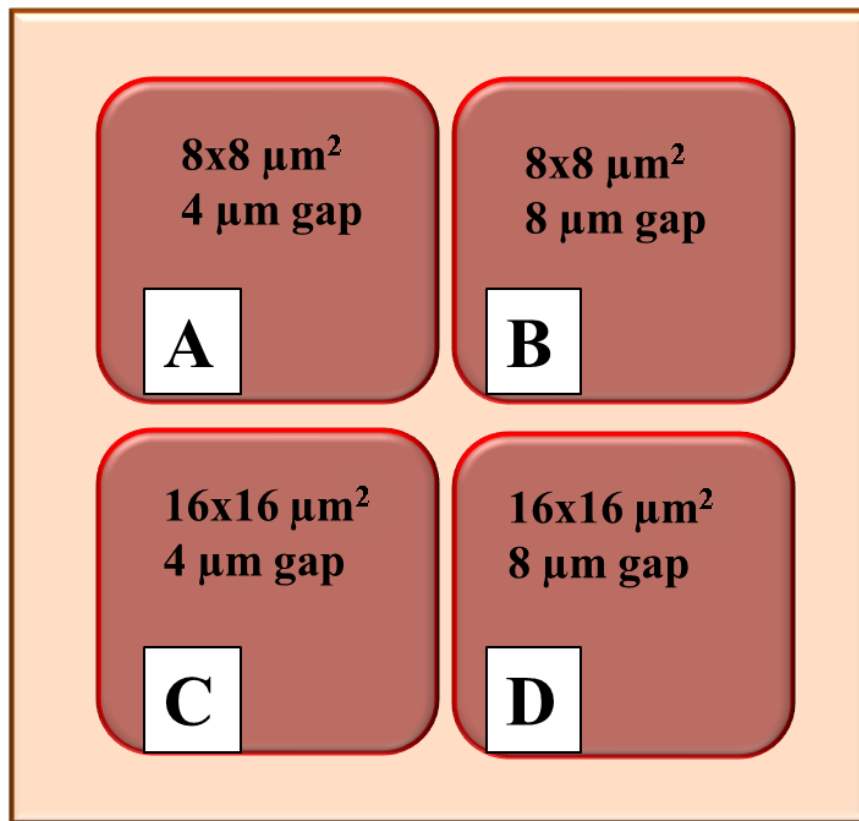


**Figure 2.1:** Image of the micropatterned silicon wafer. Silicon wafer contains 16 different patterned areas of which 4 were used in this study. Post sizes on these areas were designed to have dimensions of 8x8 µm² and 16x16 µm² with spacings of 4 µm and 8 µm and post height of 5 µm. A) 8x8 µm², gap 4 µm, B) 8x8 µm², gap 8 µm, C) 16x16 µm², gap 4 µm, D) 16x16 µm², gap 8 µm.

### 2.2.4 Preparation of Polydimethylsiloxane (PDMS) Mold

PDMS molds were prepared by weighing Sylgard 184 silicone polymer and Sylgard 184 Curing agent in a ratio of 10:1 (w/w). This mixture was stored under vacuum at ca. -200 mm Hg for 45 min. at R.T. to remove the bubbles. The mixture was then poured onto the wafers and maintained at 70 °C for 3 h in the oven. With this approach a negative copy of the original wafer was obtained.

### 2.2.5 Preparation of Micropatterned Films

By using the negative copy of the original wafer or the template, collagen-based films were prepared using solvent casting. Collagen and collagen/ELR solutions were poured into the template and air dried for 3-5 days at room temperature. The dry films were removed from the PDMS template and stored at 4 °C until use.

#### 2.2.5.1 Micropatterned Collagen Film

Collagen solution (3 mL, 15 mg/mL in 0.5 M acetic acid) was poured onto the patterned PDMS template and the film was prepared as explained above.

#### 2.2.5.2 Micropatterned Collagen/ELR film

Collagen and ELR mixture in 10:1 and 5:1 (w/w) ratio were dissolved (15 mg/mL in 0.5 M acetic acid) and 3 mL of this solution was poured onto the patterned PDMS templates. Airdried films were removed and stored at 4 °C.

### 2.2.6 Crosslinking of the Films

The collagen based micropatterned films were crosslinked physically by dehydrothermal treatment (DHT) and chemically by glutaraldehyde solution. The films were incubated at 150 °C for 24 h under vacuum (Vacuum Oven Model 281A, Cole-Parmer, USA) and then maintained in 1% glutaraldehyde solution for 30 min. The films were washed excessivelly with distilled water and stored in PBS until use.

### 2.2.7    Characterization of the Films

Films pillar dimensions were characterized by analyzing their SEM micrographs (SNE 3000M SEC, Korea) with NIH ImageJ.

### 2.2.8    In vitro Studies

### 2.2.8.1 Sterilization of the Films

Crosslinked films were sterilized by 70% ethanol in a laminar flow hood for 3 h at room temperature. Then they were washed with sterile PBS (0.1 M, pH 7.4) 3 times.

### 2.2.8.2 Saos-2 human Osteosarcoma Cell Culture

Saos-2 cells (ATCC No: HTB-85) were stored frozen in their medium and 15% DMSO, at - 196 °C. Cells were cultured in RPMI 1640 medium supplemented with 10% fetal bovine serum (FBS), 100 U/mL penicillin, 100 µg/mL streptomycin, 1 µg/mL amphotericin B, and 10 µg/mL vancomycin. Cells were cultured in a $CO_2$ incubator at 37 °C, and 5% $CO_2$. Growth medium was changed every two days. The cells were removed from the culture flasks with Trypsin-EDTA, diluted to 0.05% from a 0.25% stock in PBS pH 7.4.

### 2.2.8.3 Cell seeding onto the Films

Films were allowed to airdry for 2-3 h to allow cell penetration. Cells were detached from the surface of flask by Trypsin-EDTA diluted to 0.05% with PBS pH 7.4 (37 °C for 5 min). Then trypsin was blocked with addition of RPMI 1640 medium and centrifuged (3000 g, 5 min). After suspending the cells in the medium, cell number was determined by using a hemocytometer. 7000 cells suspended in 50 µL of RPMI 1640 growth medium were seeded per area of film (64 mm$^2$). After allowing the cells to adhere for 3 h, 5 mL of RMPI 1640 growth medium was added into each well of 6 well plate and plates were incubated at 37 °C and 5% $CO_2$. Medium was changed every two days.

### 2.2.8.4 Determination of Alkaline Phosphatase (ALP) Activity

In order to determine the amount of ALP produced by the cells, the cell seeded films and cells on TCPs were washed with PBS (pH 7.4) and then washed again with 1X lysis buffer (1X of component B) of SensoLyte pNPP Alkaline Phosphatase Assay Kit (Anaspec, USA). Then, the films were transferred to a 15 mL falcon tube. 40 µL of Triton X-100 (component D) and 20 µL component B (1X) was added into the falcon tube and mixed well. More component B (1X) was added until covering the films in the falcon tubes. Content was

frozen at -20 °C and thawed at 37 °C and this step was repeated 3 times. Thawed products were sonicated at 25W on ice until the films were fragmented. After sonication, lysate was centrifuged (2000 rpm for 10 min). Then the supernatant was stored for further steps and the pellet was discarded. 50 μL of the supernatant containing alkaline phosphatase (ALP) was taken from each sample and put into the wells of 96 well plate with triplicates. ALP dilution buffer (1X of component B, 1mg/mL BSA) was used to dilute the samples in 1:1 ratio. 50 μL of pNPP substrate (component A) was added to each well and the reagents were shaken for 30 s. Then they were incubated for 1 h at 37 °C. Finally, 50 μL of stop solution (component C) was added into each well and the plate was shaken for 20 s before measuring the absorbance. Absorbance was measured at 405 nm with ELISA plate reader (Molecular Devices, USA). ALP activity was calculated by using the calibration curve. Calibration curve was prepared by using component E (alkaline phosphatase standard, 10 μg/mL). Component E was diluted to 0.2 μg/mL with ALP dilution buffer to obtain 2X serial dilutions, 200, 100, 50, 25, 12.5, 6.2, 3.1, 0 ng/mL ALP standards in ependorf tubes. From each dilution sample, 50 μL was taken and put into the wells of 96 well plate then they were incubated for 1 h at 37 °C. 50 μL of component C was added into each well and the plate was shaken for 20 s before measuring. Absorbance was measured at 405 nm with ELISA plate reader.

### 2.2.9   Microscopical Studies

### 2.2.9.1 Fluorescence Microscopy

### 2.2.9.1.1        DAPI Staining

Films were prepared for staining on day 1 and 14 of seeding. Medium was discarded and the cells were fixed with 4% (w/v) paraformaldehyde at room temperature for 30 min. Cell membrane was permeabilized with Triton X-100 (1% v/v in PBS pH 7.4) at room temperature for 5 min. After washing twice, samples were incubated in BSA (1% w/v in PBS) at 37 °C for 30 min. After washing three times with 0.1% BSA, the samples were incubated with DAPI (1:3000 w/v, in 0.1% BSA) for 5 min at 37 °C. Samples were washed with PBS three times and stored in PBS solution until examination using a Zeiss Axio Imager M2 (Germany) fluorescence microscope.

### 2.2.9.2 Scanning Electron Microscopy (SEM)

Films were examined with SEM on the day 1 and day 14 of seeding. Films were washed twice with PBS and cacodylate buffer (0.1 M, pH 7.4). They were fixed with 2.5% v/v glutaraldehyde in cacodylate buffer for 2 h at room temperature. After washing again with cacodylate buffer, the films were freeze dried for 3 h (Karnovsky, 1965). Before examination with SEM, surfaces of the films were coated with Au under vacuum.

### 2.2.9.3 Computerized Analysis of Microscopy Images

Fluorescence micrographs were analyzed with Image J (NIH, USA) to determine the number of cells, degree of nuclear deformation, perimeter of the nucleus, and circularity of the nucleus for each pattern type. For cell number analysis, 5 random areas were counted and total cell number was calculated according to the ratio between total area and area used for cell counting. For all nuclei deformation analysis, 5 random areas with a cell number around 100 were used.

### 2.2.10 Statistical Analysis

Statistical analysis was carried out by using a Student's t-test with a minimum confidence level of 95% (p value lower than 0.05) for statistical significance.

# CHAPTER 3

# RESULTS AND DISCUSSION

## 3.1 Characterization of Isolated Collagen

Collagen type I was isolated from tail skins of the Spraque-Dawley rats as described in Section 1.2.1 and the purity of the collagen was studied with SDS-PAGE as described in Section 1.2.1.1. In the Figure 3.1, there are three lanes showing protein ladder (Fermentas), the commercial collagen type I (Sigma, Germany) and the isolated collagen respectively. Commercial collagen type I (lane II) presents two bands, around 260 kDa and 140 kDa. The collagen isolated collagen in this study presents the same bands with the commercial collagen, and this shows that isolated collagen is a type I collagen. Also, there are no other bands for isolated collagen which also indicate that the isolated collagen is pure.
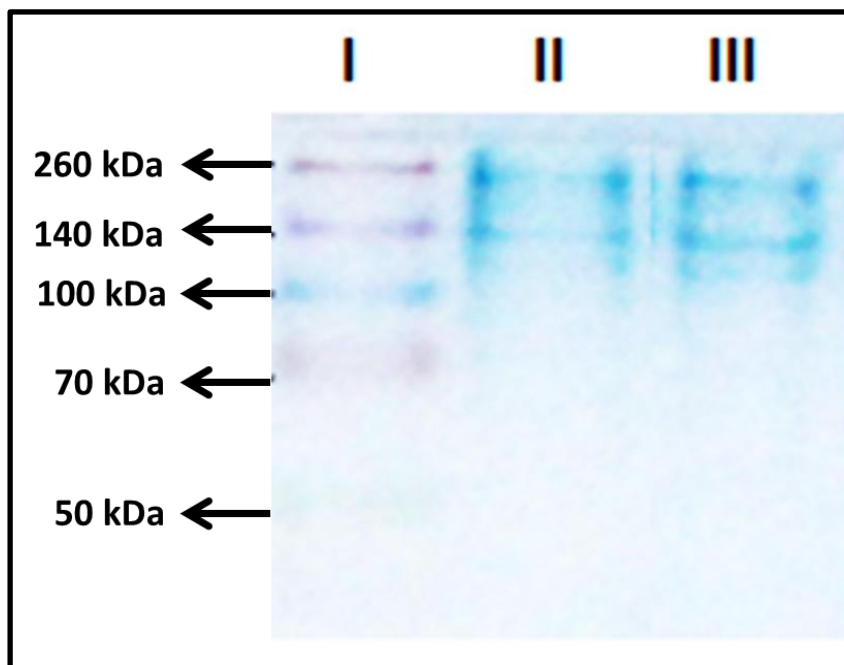


**Figure 3.1** SDS-PAGE result of collagen isolated from rat tail tendons. Lanes I, II and III represent the protein ladder (Fermentas), commercial collagen type I (Sigma, Germany) and the isolated collagen, respectively.

## 3.2 Surface Characterization of the Films

Micropillar covered wafers were prepared as described in Section 1.2.3 and served as the main template. Then, by using PDMS replica (inverse template) of these wafers as in Section 1.2.4, micropatterned collagen and ELR films were obtained as mentioned in Section 1.2.5.1. Pillar geometries and dimensions of the wafers were predetermined and the design involved 4 regions covered with 8x8 µm² and 16x16 µm² pillars separated by either 4 or 8 µm gaps with a height of 5 µ (Figure 3.2). The SEM micrographs in Figure 3.2 were taken with a 31.6° tilt angle. Actual wafers were not observed since SEM sample preparation requires surface coating with gold and it would not be possible to use them again. There were no micrographs of pillars with 4 µm gap since they cannot be observed with the microscope well due to the size of the gaps.
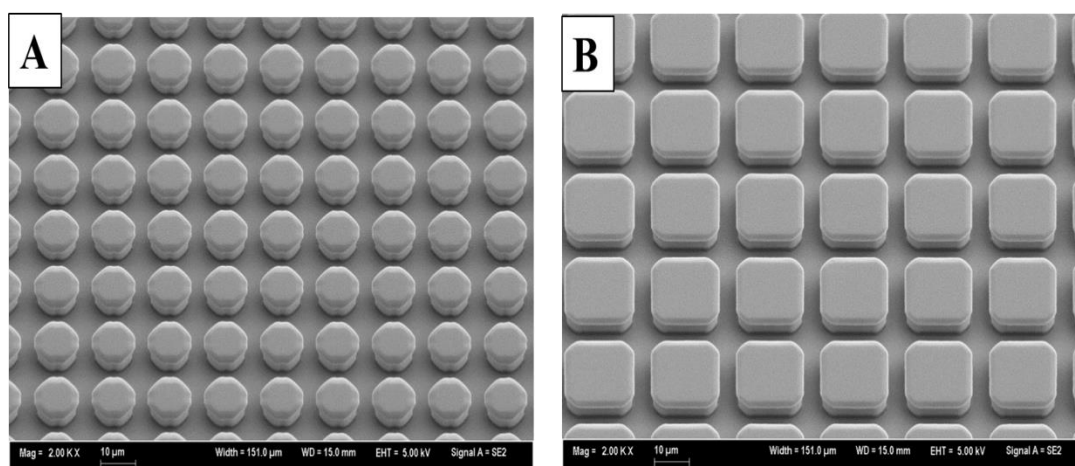


**Figure 3.2** SEM micrographs of the main template with 5 µm micropillar height. Tilt angle of the stab: 31.6°. A) 8x8 µm², gap 8 µm, B) 16x16 µm², gap 8 µm. Magnification (x2000).

After the preparation of the main template wafers, micrographs were taken by light microscope (Figure 3.3). There were deviations from the expected pillar sizes. These deviations may be due to low throughput capability of the laser lithography method used in the production of wafers (Chauvy et al, 2003). Instead of laser lithography, electron beam lithography can be used for further development of the constructs because EBL offers high resolution and quality as mentioned in Section 1.2.3 (McMurray et al, 2011). Also, after the seeding of cells onto the film surfaces, micrographs of the film surfaces were taken on the 1st day and 14th day of the seeding with a fluorescence microscope (Zeiss Axio Imager M2, German). Especially, on the 14th day of culture, it was observed that pillars get bigger and

the gaps between them get smaller (Table 3.2, 3.3 and 3.4). This deformation can be a result of long duration time in medium during culturing and in PBS after staining procedure.
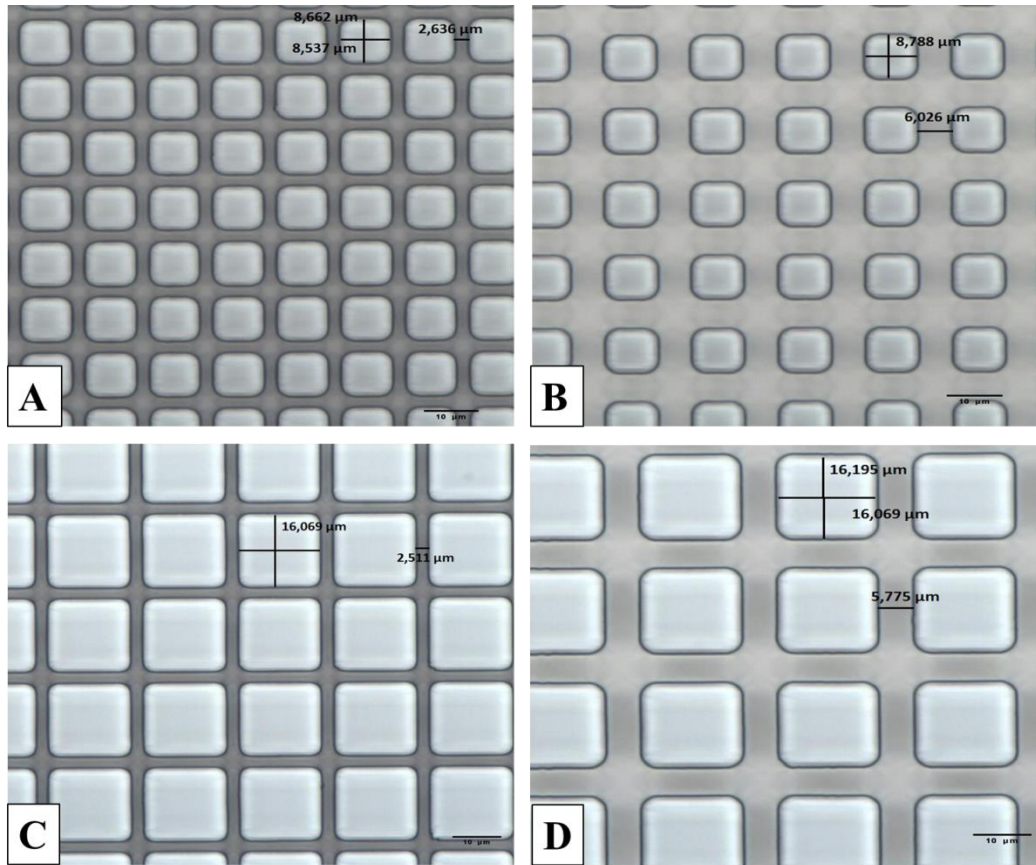


**Figure 3.3** Pillars on the silicon wafers. A) 8.54x8.66 µm², 2.64 µm gap, B) 8.79x8.79 µm², 6.07 µm gap, C) 16.07x16.07 µm², 2.51 µm gap, D) 16.20x 16.07 µm², 5.78 µm gap. Pillar heights were 6.30 µm. Micrographs were taken by light microscope. Magnification (x50). Scale bars: 10 µm.

**Table 3.1** Pillar dimensions designed and obtained.

|   | Designed dimensions (μm) | Obtained area (μm²) | Obtained gap length (μm) |
|---|---|---|---|
| A | 8x8 μm², gap 4 | 8.54±0.26 x 8.66±0.22 | 2.64±0.19 |
| B | 8x8 μm², gap 8 | 8.79±0.24 x 8.79±0.27 | 6.07±0.21 |
| C | 16x16 μm², gap 4 | 16.07±0.27 x 16.07±0.23 | 2.51±0.15 |
| D | 16x16 μm², gap 8 | 16.20±0.32 x 16.07±0.34 | 5.78±0.17 |

There are three types of films used in this study as mentioned in Sections 1.2.5.1 and 1.2.5.2: Pure collagen, collagen:ELR (1:0.1) and collagen:ELR (1:0.2). When these films were compared with each other in terms of pillar deformation, no significant difference was observed between them (Tables 3.2, 3.3 and 3.4). However, for all types of the films, it can be said that pillar dimensions changed during 14 days of culture. Pillars were bigger and the gaps were smaller than before seeding for all types of films, although films were crosslinked with dehydrothermal treatment (DHT) (150°C, 24 h under vacuum) and with glutaraldehyde (in 1% glutaraldehyde solution for 30 min). This may be a result of storing the films in PBS for 4-5 days after the fixation of the cells on the $14^{th}$ day of the culture for microscopic studies.

**Table 3.2** Pillar dimensions after cell seeding for pure collagen films

|   | Obtained area (μm²), $1^{st}$ day of culture | Obtained gap length (μm), $1^{st}$ day of culture | Obtained area (μm²), $14^{th}$ day of culture | Obtained gap length (μm), $14^{th}$ day of culture |
|---|---|---|---|---|
| A | 8.62±0.26 x 8.76±0.22 | 2.51±0.65 | 8.94±0.60 x 8.81±0.56 | 2.27±0.76 |
| B | 8.94±1.02 x 8.65±0.50 | 6.00±0.61 | 9.00±0.94 x 8.81±0.86 | 5.81±0.50 |
| C | 16.35±0.23 x 16.08±1.08 | 3.54±0.59 | 17.53±0.29 x 16.94±0.75 | 1.67±0.38 |
| D | 16.43±0.89 x 16.47±1.00 | 6.17±1.00 | 16.47±0.55 x 16.65±0.19 | 6.03±0.48 |

**Table 3.3** Pillar dimensions after cell seeding for collagen:ELR (1:0.1) films

| | Obtained area (μm²), 1st day of culture | Obtained gap length (μm), 1st day of culture | Obtained area (μm²), 14th day of culture | Obtained gap length (μm), 1st day of culture |
|---|---|---|---|---|
| A | 8.34±0.11 x 8.40±0.89 | 2.91±0.29 | 8.40±0.89 x8.47±0.30 | 2.55±0.20 |
| B | 8.94±0.59 x 8.41±0.77 | 6.41±0.75 | 9.31±0.97 x 9.42±0.57 | 6.28±0.44 |
| C | 16.14±0.98 x 16.08±0.15 | 3.74±0.29 | 17.87±0.56 x 17.21±0.55 | 2.13±0.56 |
| D | 16.13±0.14 x 16.28±0.64 | 6.12±0.67 | 16.67±0.66 x 16.81±0.88 | 6.03±0.60 |

**Table 3.4** Pillar dimensions after cell seeding for collagen:ELR (1:0.2) films

| | Obtained area (μm²), 1st day of culture | Obtained gap length (μm), 1st day of culture | Obtained area (μm²), 14th day of culture | Obtained gap length (μm), 1st day of culture |
|---|---|---|---|---|
| A | 8.29±0.91 x 8.37±0.81 | 3.37±0.30 | 10.04±0.59 x 9.63±0.46 | 2.47±0.42 |
| B | 7.93±0.37 x 8.14±0.49 | 6.55±0.74 | 9.47±0.87 x 9.47±0.56 | 5.67±0.24 |
| C | 16.31±0.62 x 16.91±0.53 | 3.30±0.59 | 17.20±0.56 x 16.80±0.87 | 2.29±0.75 |
| D | 16.21±0.56 x 16.31±0.39 | 6.94±0.60 | 16.81±0.30 x 16.67±0.67 | 5.00±0.41 |

## 3.3 In vitro Studies

### 3.3.1    Cell Adhesion

In this study, cell numbers were counted on the fluorescence micrographs of the nuclei. 5 random areas are counted and total cell number was calculated according to the ratio between total area and area used for cell counting (Figure 3.4). However, there is no significant difference in between the different surfaces (pure collagen, collagen:ELR (1:0.1) and collagen:ELR (1:0.2)) in terms of the cell number. Studies show that surface physical

properties are more dominant on the cell behavior than the surface mechanical or chemical properties. So, independent from the surface chemistry or mechanics, surface topography can affect the cell behavior (Davidson et al, 2010; Pan et al, 2012, Badique et al, 2013). Similarly, according to the results of this study, although the composition of the surfaces did not affect the cell number, micropillar dimensions seem to be affecting the number of cells. Cell numbers were the least at area B which has the lowest pillar size with highest gap (8x8 $\mu m^2$, gap 8 $\mu m$) (Figure 3.4).  Also B area is the area that the most deformation of the cells was observed (Figure 3.16). Finally, the cell numbers are higher for unpatterned surfaces. It seems that cells prefer unpatterned surfaces. This result is similar with the studies in the literature. For example, in a study, human embryonic stem cells show a reduction in proliferation on nanopatterned substrates (Gerecht et al, 2007). Also, in another study, various cell types and nanotopographies were used and it was observed that cells show reduced proliferation on nanotopographical surfaces compared to smooth, unpatterned surfaces (Bettinger et al, 2009).

Another property studied in this study was material stiffness. Normally stiffness is a mechanical property affecting cell behavior on the substrate surfaces. In the literature, there are several studies on stiffness. For example, when mesenchymal stem cells were grown on rigid gels, differentiation through muscle forming was observed due to the elasticity of the gel similar to the muscle. Also, when the neural stem cells were seeded on soft scaffolds having similar mechanical property with normal brain tissue, neuron differentiation was observed (O'Brien, 2011). Moreover, studies show that ELR used in the films also affects cell proliferation and stiffness of the substrates. RGD sequences in the structure of ELR is used to improve cell adhesion (Kinikoglu et al, 2011) but ELR incorporation also decreases the compressive strength and stiffness of the collagen films (Arias et al, 2006). These examples indicate that the substrate mechanical property is important for the cell behavior. In this study, it was aimed to see the ELR effect on cell adhesion, proliferation and conformational change. For this reason, three types of films were used as pure collagen, collagen:ELR (1:0.1) and collagen:ELR (1:0.2). However, there was no consistent difference between the three types of films. Probably, it was a result of low ELR content in the collagen/ELR composing films, and this low content of ELR was not enough to change the mechanical properties between the films significantly. Similarly, in a study Garcia et al. (2009) show that the mechanical properties between the scaffolds which were composed of 100:0 (Collagen:ELR) and 75:25 (Collagen:ELR) were not significant and not evident statistically. However, when they used highly different amounts of ELR containing scaffolds such as 50:50 and 25:75 (Collagen:ELR) ratios and compared each with pure collagen films, they observed significant mechanical property changes.

Finally, for the 14th day of the culture, it was observed that there is almost no cell on the micropillar surfaces but there were a number of cells on the middle of the films which has no micropillar. This may be due to the changes in micropillar sizes and deformations in the pillar geometries after storing the films in PBS for 4-5 days after fixation or PBS may disrupt the cells.
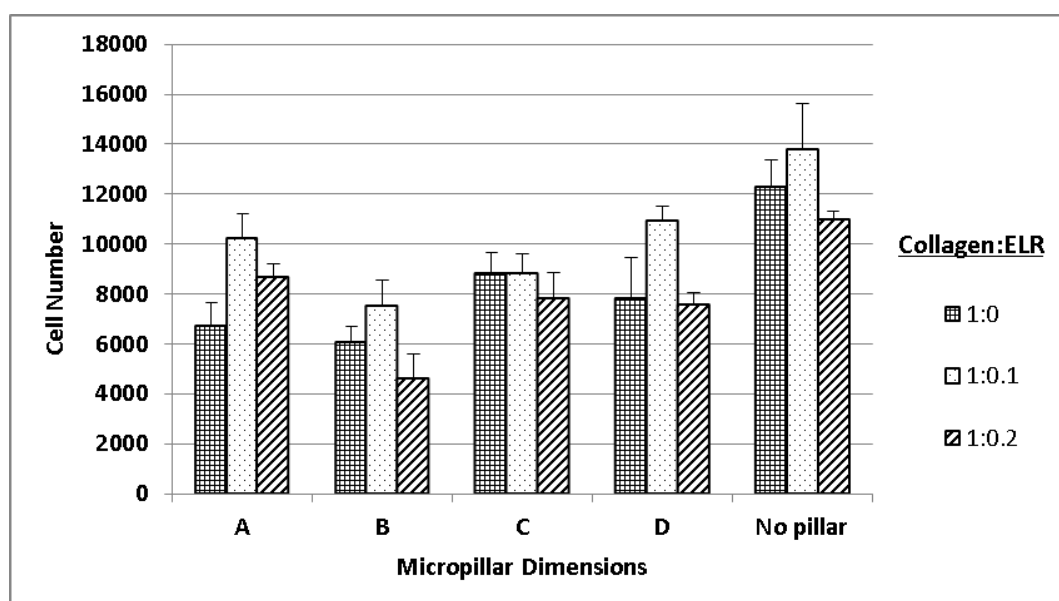
**Figure 3.4** Cell number after 1$^{st}$ day of culture for all types of films. (7000 cells were seeded for each area). A) 8x8 μm², gap 4 μm, B) 8x8 μm², gap 8 μm, C) 16x16 μm², gap 4 μm, D) 16x16 μm², gap 8 μm.

**Table 3.5** Cell number statistical analysis for pure collagen, collagen:ELR (1:0.1), collagen:ELR (1:0.2) films

| Template type | Significance compared to B | Significance compared to no pillar |
|:---:|:---:|:---:|
| A | * | ** |
| B | - | ** |
| C | * | ** |
| D | * | ** |
| No pillar | * | - |

\* Cell number on B area is significantly lower than the others (Student's t-test with a minimum confidence level of 95%, p value lower than 0.05)

\*\* Cell number on unpatterned (no pillar) area is significantly higher than the others (Student's t-test with a minimum confidence level of 95%, p value lower than 0.05)

35

### 3.3.2 Alkaline Phosphatase Activity of the Cells

Alkaline phosphatase is an extracellular enzyme and it is secreted by osteoblasts during early mineralization activity of the cells. At the mineralization stage, ALP provides inorganic phosphate for hydroxyapatite crystal nucleation by hydrolyzing phosphate (Wuthier et al., 1982). During osteoblast development, down regulation of proliferation is observed and cells are ALP positive which indicates osteoblastic differentiation (Stein et al, 1993). Finally, a recent study reported that ALP activity on the 7th day of Saos-2 cell culture is higher when HRGD-6 sequence containing ELP surfaces were used compared to ELP with no RGD sequences or chitosan surfaces with no ELP (Costa et al, 2009).

Another parameter affecting the ALP activity was found to be the topography of the surfaces. Studies show that nanostructures cause differentiation of mesenchymal stem cells into osteoblast without any other promoters (Dalby et al, 2006; Dalby et al, 2007). Another study reported an increase in ALP of marrow stromal cells on nanoporous alumina substrates when compared to amorphous alumina surfaces with no nanoarchitecture (Popat et al, 2007). ALP activity was observed in human mesenchymal stem cells (hMSCs) after 2 weeks of culture on micropost arrays with diameter of about 2 μm, heights of 1–12 μm and spacing of 4 μm between the microposts. Also on the 7th day of the culture, hMSCs on microposts showed osteogenic differentiation (ALP activity) possibly due to microposts (Fu et al, 2010). In this study, TCP and micropatterned films with ELRs and collagen were seeded with Saos-2 cells and ALP activity of the cells were determined on the 14th day of the culture in order to see the effect of micropatterns and ELR on cell activity (Figure 3.5). In terms of ELR content of the films, results showed that the highest ALP activity on the films with the highest ELR ratio. This result was consistent with the literature that the ELR containing HRGD-6 sequences cause the highest cell activity (Costa et al, 2009). On the other hand, in terms of micropillar distributions, ALP activity of the Saos-2 cells on the B area was higher than on all the other areas. B is the area which also caused the most deformation of the cells. However, TCPs showed the most ALP activity (Figure 3.5). This was probably due to the higher cell number on this surface since the unpatterned area had the highest cell number for all types of the films (Figure 3.4).
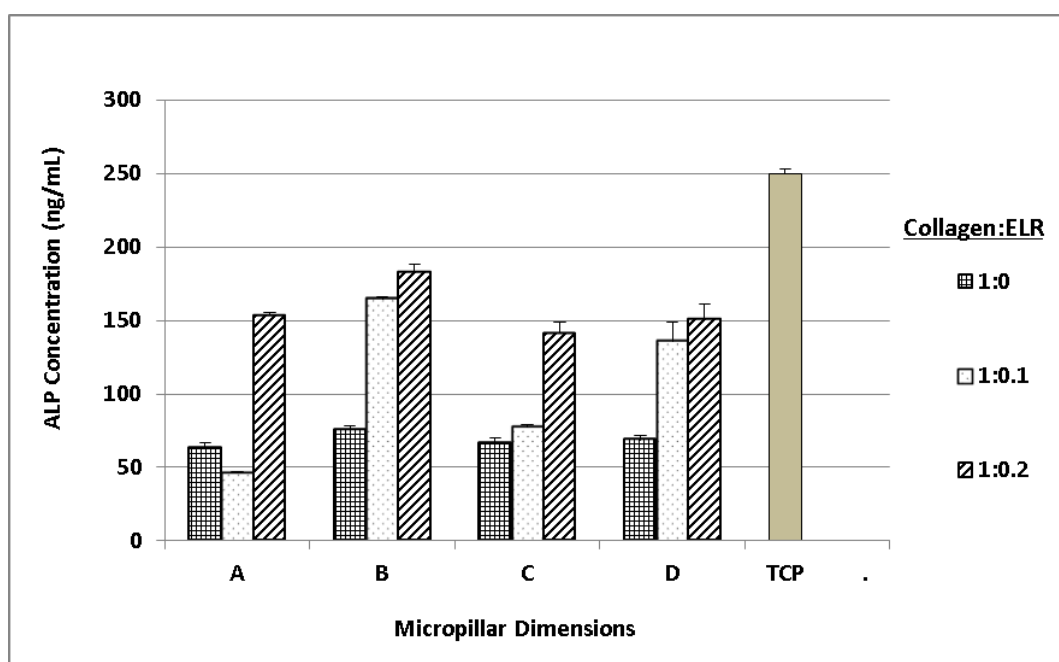
**Figure 3.5** ALP activities of Saos-2 cells on 14th day of the culture. A) 8x8 µm², gap 4 µm, B) 8x8 µm², gap 8 µm, C) 16x16 µm², gap 4 µm, D) 16x16 µm², gap 8 µm.

**Table 3.6** ALP concentration statistical analysis for pure collagen, collagen:ELR (1:0.1), collagen:ELR (1:0.2) films

| Template type | Significance compared to B (1:0 Coll:ELR) | Significance compared to B (1:0.1 Coll:ELR) | Significance compared to B (1:0.2 Coll:ELR) | Significance compared to TCP |
|---|---|---|---|---|
| A | * | * | ** | *** |
| B | - | - | - | *** |
| C | * | * | ** | *** |
| D | * | * | ** | *** |
| TCP | * | * | ** | - |

\* ALP concentration on B areas are significantly higher than the other areas (Student's t-test with a minimum confidence level of 95%, p value lower than 0.05)

\*\* ALP concentration on B area for ELR:collagen (1:0.2) film is higher than the B areas on the other film (Student's t-test with a minimum confidence level of 95%, p value lower than 0.05)

\*\*\* ALP concentration on TCP is significantly higher than the patterned areas (Student's t-test with a minimum confidence level of 95%, p value lower than 0.05)

### 3.3.3 Cell Conformational Change

### 3.3.3.1 Study of Deformation of Cell Morphology and Nucleus

Saos-2 cells were cultured on the micropatterned films and the deformation of the nucleus and cytoskeleton were studied. Cells were observed under fluorescence microscopy on the 1$^{st}$ and 14$^{th}$ day of the culture. It was observed that cells and their nuclei are deformed on the micropillar covered surfaces on all types of films (Figures 3.6, 3.7, and 3.8). ELR and collagen content of the films did not seem to affect nuclei deformation (Figures 3.16, 3.17 and 3.18). However, pillar placement and dimensions seem to be effective on the nuclei shapes. Micrographs show that nuclei of the cells fall in the gaps when the gaps are large enough (Figures 3.6.B and D, Figures 3.7.B and D, Figures 3.8.B and D). When the gaps were smaller, nuclei were observed mostly on the pillar surfaces instead of the gaps (Figures 3.6.A and C, 3.7.A and C, and 3.8.A and C). These results are also consistent with the studies in the literature. In a study, a relation between micropillar size and Saos-2 cell nuclei deformation was studied (Badique et al, 2013). Poly(L-lactide) (PLLA ) pillar gaps 2-4 µm, 5-10 µm, and 11-21 µm were used to study the degree of the nucleus deformation. Gaps 2-4 µm showed that the cells were not able to occupy the gap between the pillars completely. For 5-10 µm pillar gaps, the cells were localized completely between the pillars and this resulted in deformations in the cytoplasmic compartments and the nucleus. For the third types of the pillar with 11-20 µm gaps, cell body deformations were very clear and the cells were completely between the gaps. However, there was almost no nuclei deformation (Badique et al, 2013).
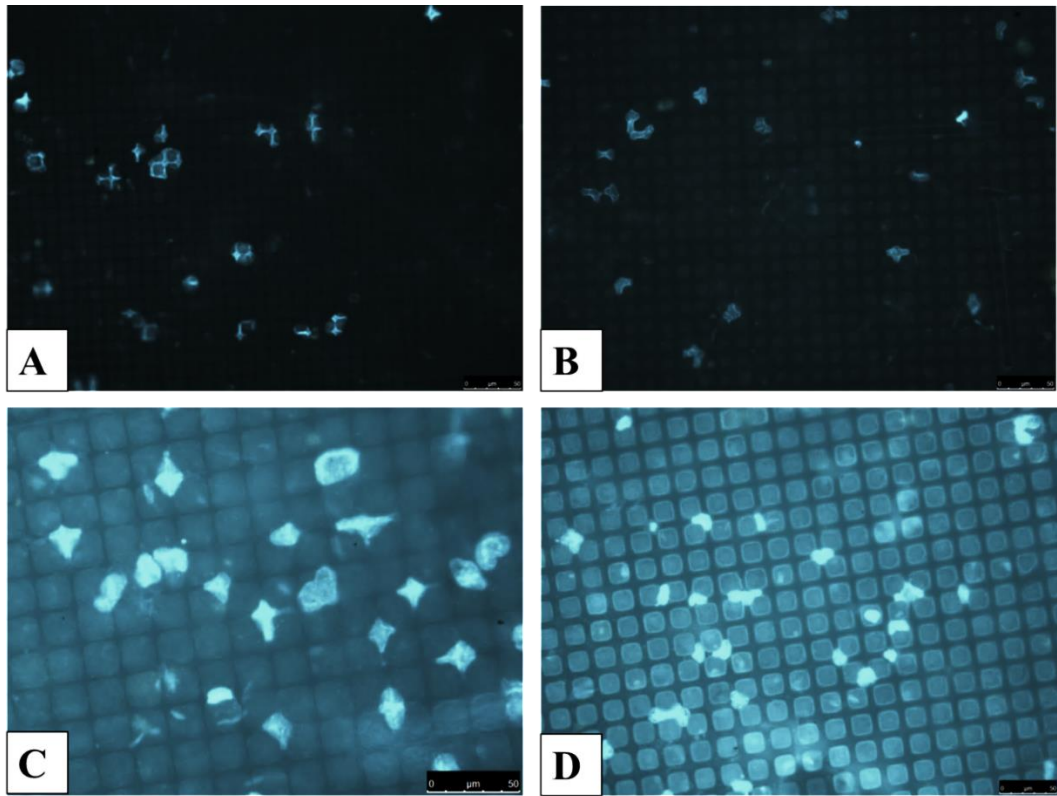
**Figure 3.6:** Saos-2 cell nucleus deformation micrographs with fluorescence microscope on pure collagen film. A) 8x8 µm², gap 4 µm, B) 8x8 µm², gap 8 µm, C) 16x16 µm², gap 4 µm, D) 16x16 µm², gap 8 µm (x20). Nuclei were stained with DAPI after 1st day of culture.
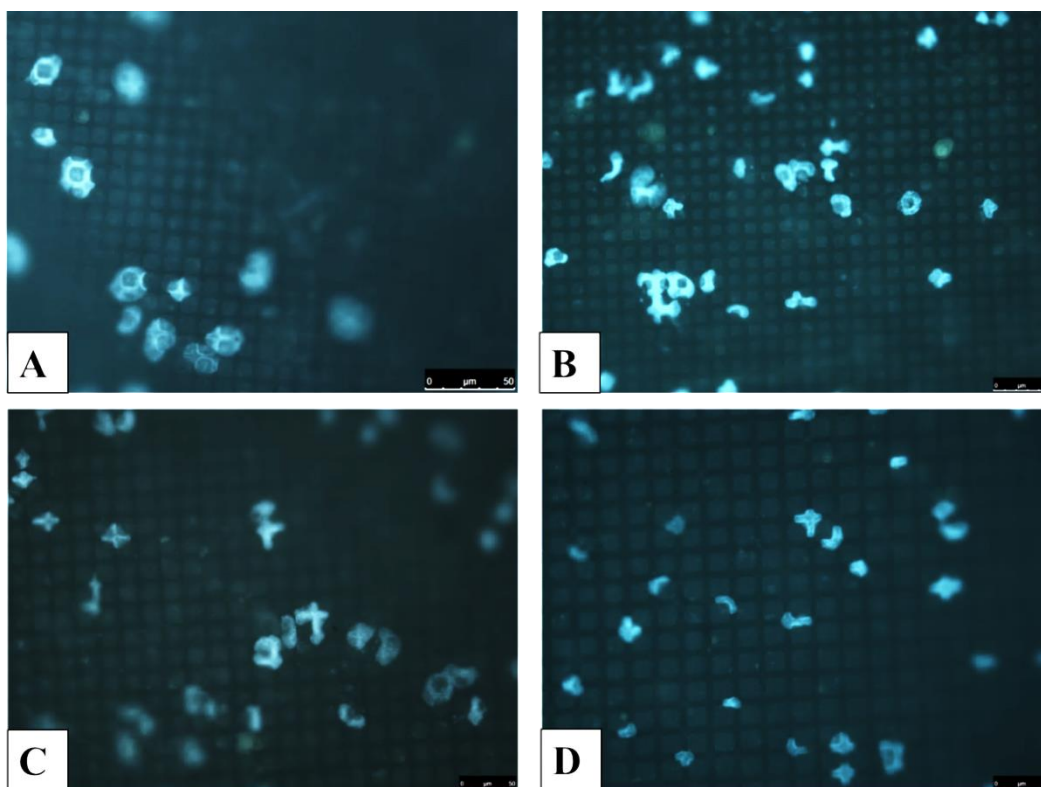
**Figure 3.7:** Saos-2 cell nucleus deformation micrographs with fluorescence microscope on collagen:ELR (1:0.1) film. A) 8x8 µm², gap 4 µm, B) 8x8 µm², gap 8 µm, C) 16x16 µm², gap 4 µm, D) 16x16 µm², gap 8 µm (x20). Nuclei were stained with DAPI after $1^{st}$ day of culture.
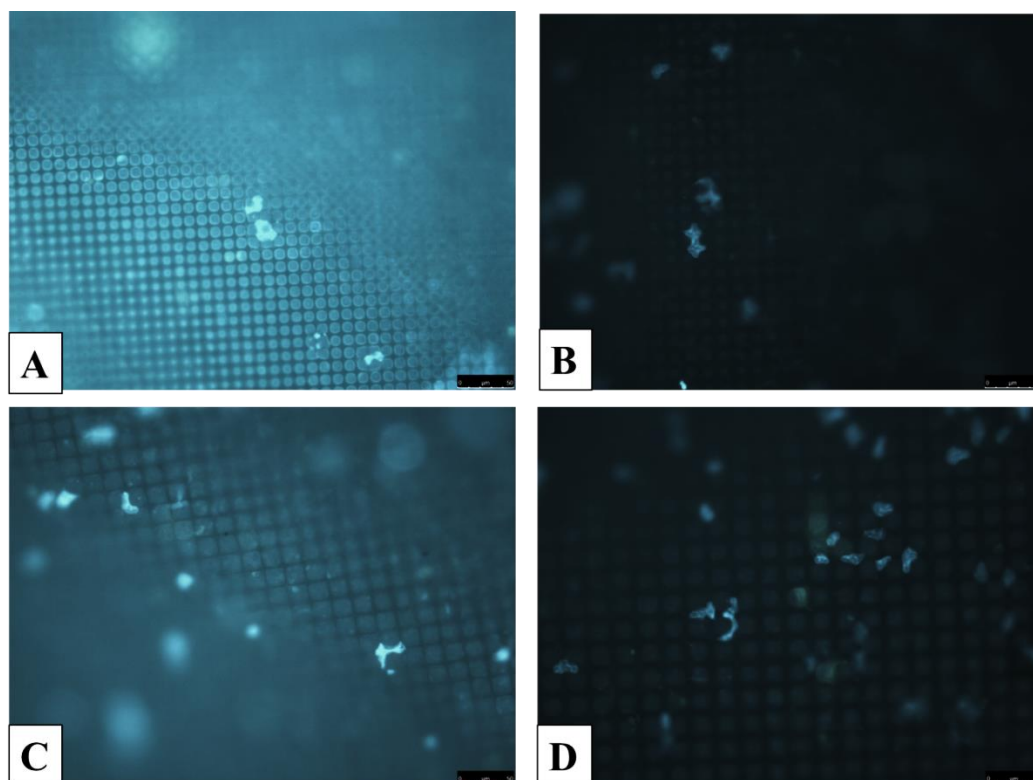
**Figure 3.8:** Saos-2 cell nucleus deformation micrographs with fluorescence microscope on collagen:ELR (1:0.2) film. A) 8x8 µm², gap 4 µm, B) 8x8 µm², gap 8 µm, C) 16x16 µm², gap 4 µm, D) 16x16 µm², gap 8 µm (x20). Nuclei were stained with DAPI after 1st day of culture.

For all types of the films, SEM micrographs of the cells show that the cells were also deformed or conformed to the shape of the pillars (Figures 3.9, 3.10 and 3.11). When the pillar dimensions were large, it can be observed that the cells stay on top of the pillars. Moreover, they were placed in between the gaps when the gaps are large and pillar dimensions were small since there is not enough space to place on top of the pillars.
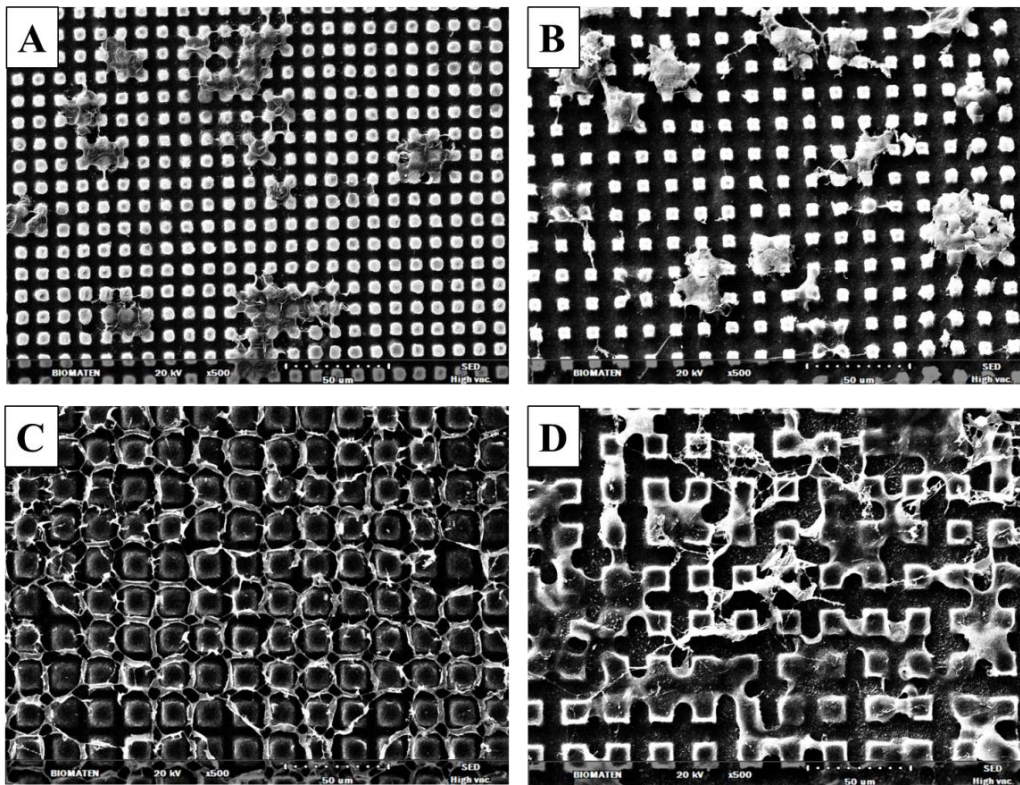
**Figure 3.9:** SEM of Saos-2 cells on pure collagen film. A) 8x8 µm², gap 4 µm, B) 8x8 µm², gap 8 µm, C) 16x16 µm², gap 4 µm, D) 16x16 µm², gap 8 µm (x500).
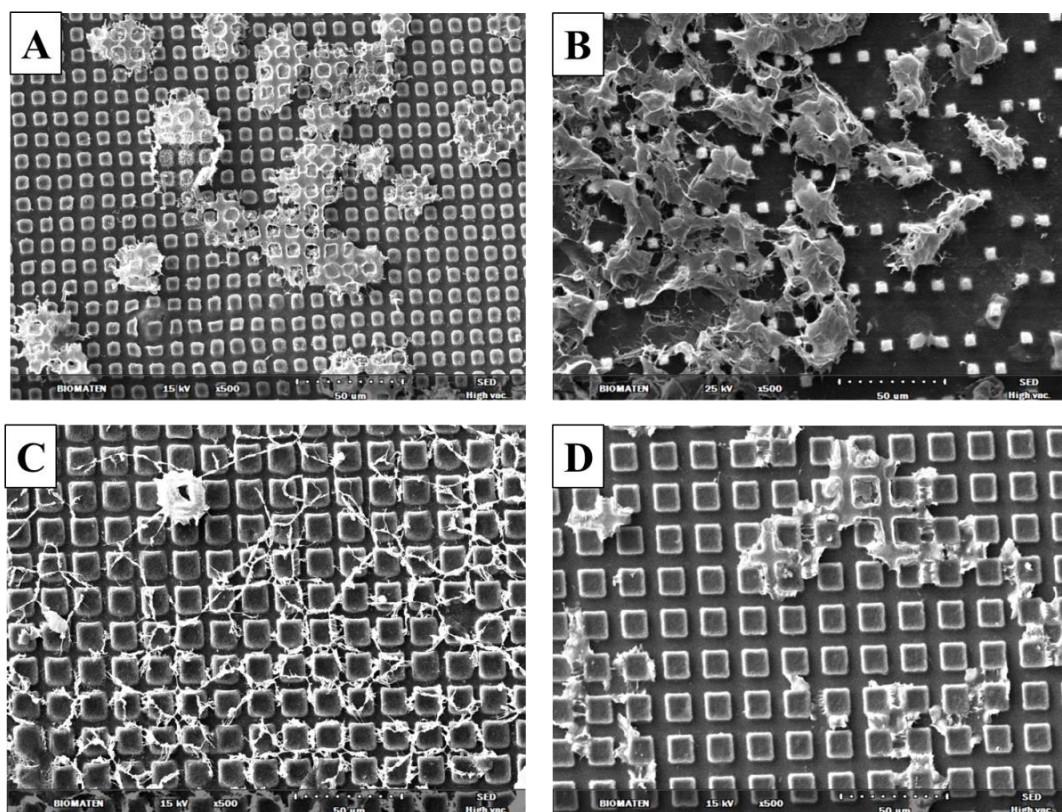
**Figure 3.10:** SEM of Saos-2 cells on collagen:ELR (1:0.1) films. A) 8x8 µm², gap 4 µm, B) 8x8 µm², gap 8 µm, C) 16x16 µm², gap 4 µm, D) 16x16 µm², gap 8 µm (x500).
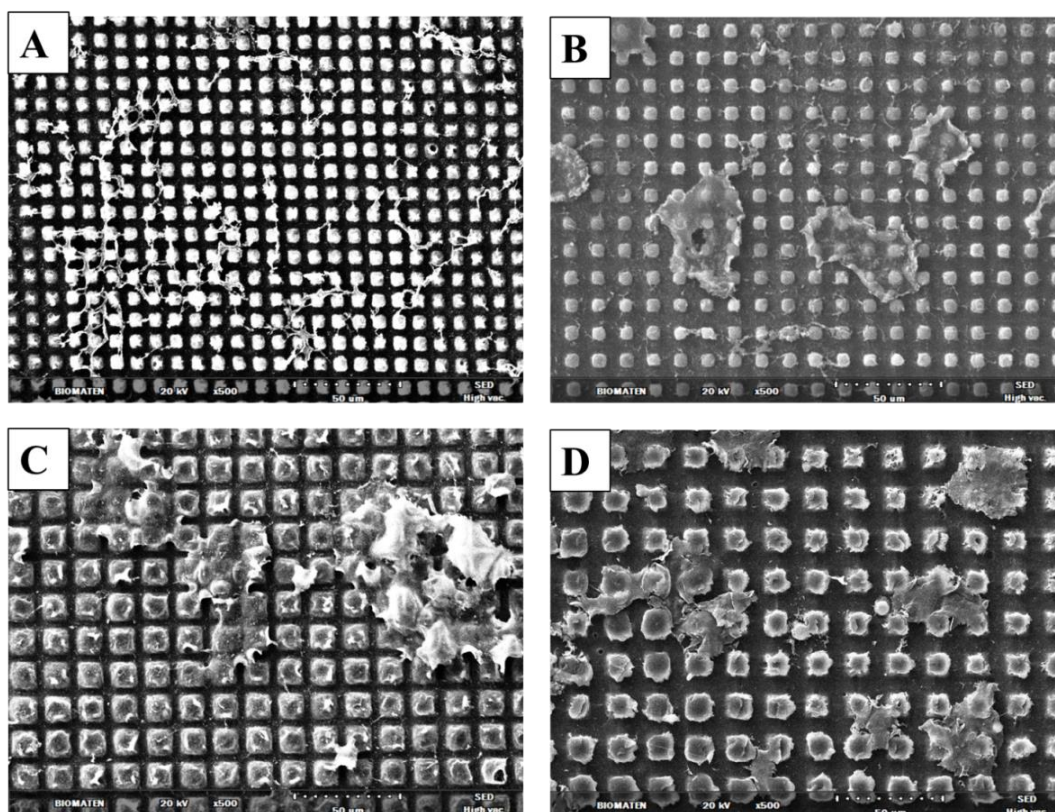
**Figure 3.11:** SEM of Saos-2 cells on collagen:ELR (1:0.2) films. A) 8x8 µm², gap 4 µm, B) 8x8 µm², gap 8 µm, C) 16x16 µm², gap 4 µm, D) 16x16 µm², gap 8 µm (x500).

Moreover, there is a consistency between the nucleus and cell deformations in terms of shape. Figures 3.12 and 3.13 show this clearly. When the cell nuclei took cross shape, cells also took the same shape with the nuclei. This study indicates that the cells on a micropatterned surface either spread on the surface due to the gap size limitations, or they deform and get the shape dictated by the surface topography. This results in deformation of the cell nucleus. Also a similar study with our research patterns indicates that the deformations were due to mechanical deformation causing bulk mass of the nucleus to be placed in between the pillars (Davidson et al, 2009). These cells are adherent cells and need large surfaces to spread on and make contact needed for mobility, cell division and other activities. When the top surfaces of the pillars are sufficiently large (comparable to that of the cell) and more importantly the gaps in between are too narrow for the cells to fit in, they stay on top. Otherwise they slip between the pillars, take contorted conformations. If the gaps were much larger, the cells would have been less contorted or more flat and spread (Davidson et al, 2009).
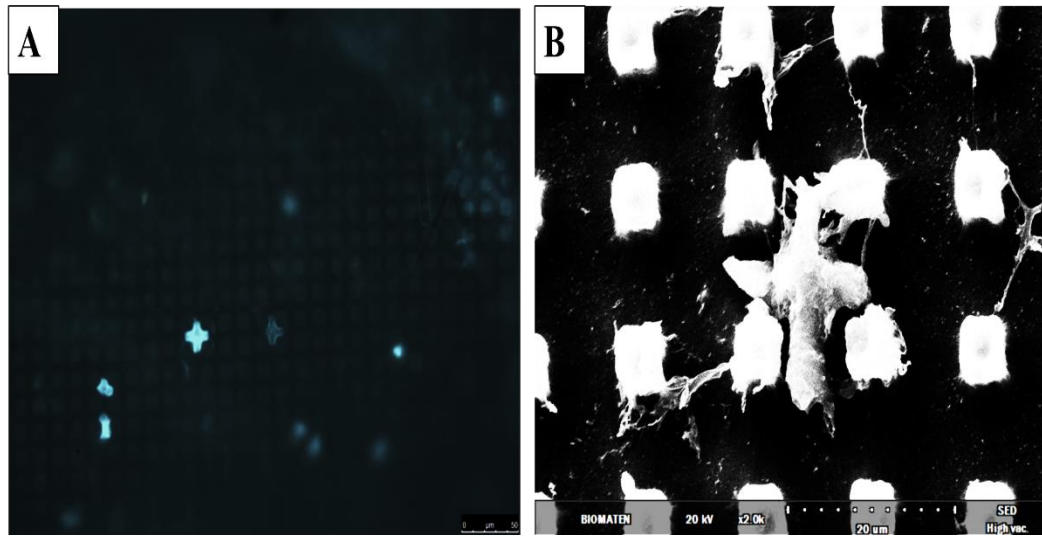
**Figure 3.12:** Saos-2 cell nucleus and cell deformation micrographs on pure collagen films with 8x8 μm², gap 8 μm pillar distribution. A) DAPI stained nuclei obtained with fluorescence microscopy (x20), B) SEM of the same cells (x2000).
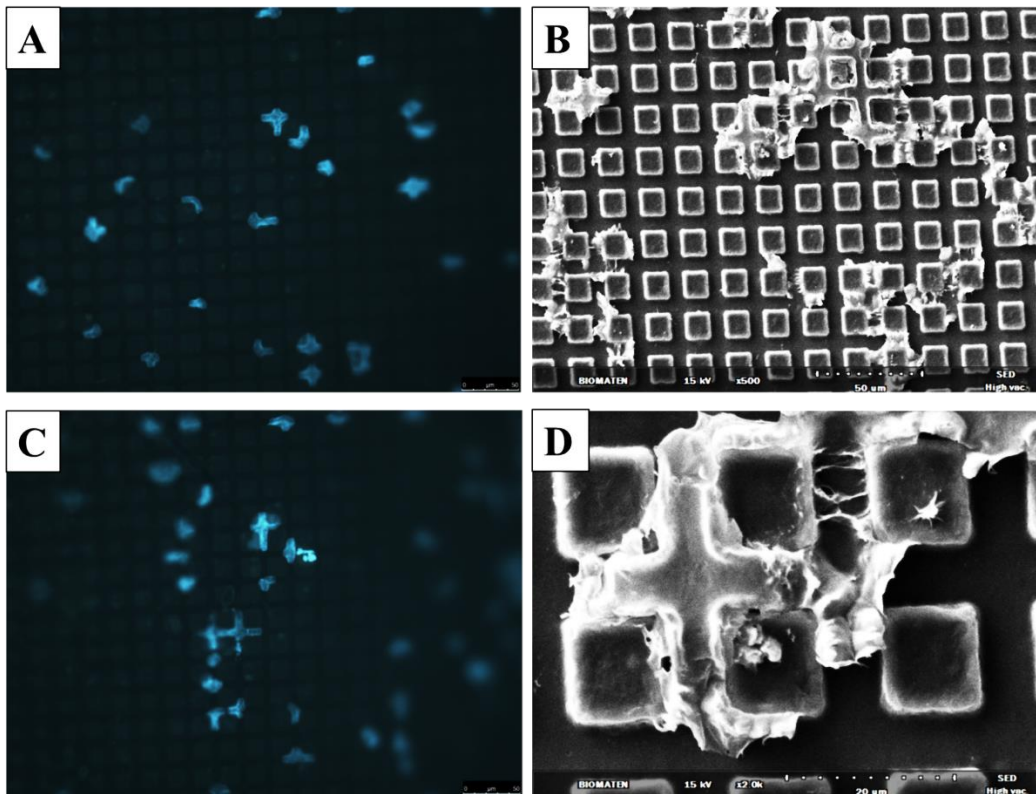
**Figure 3.13:** Saos-2 cell nucleus and cell deformation micrographs on collagen:ELR (1:0.1) films with 16x16 µm², gap 8 µm pillar distributions. A), C) DAPI stained nuclei obtained with fluorescence microscope (x20), B) SEM micrograph (x500), D) SEM micrograph (x2000).

Finally, another evidence of cell nucleus and cell deformation due to the pillars on the films was proved by comparing pillar covered surfaces with unpatterned surfaces of the films. Figure 3.14 shows the micrographs taken from the area both the patterned and unpatterned surfaces are seen. Figure 3.15 shows the cell and nucleus behaviors on unpatterned surfaces. It can be said with certainty that there is no cell deformation on the smooth, unpatterned surfaces and the reason of the deformations was the pillars on the film surfaces. Also, Figure 3.15.B and D shows the formation of a cell sheet on the smooth surfaces.
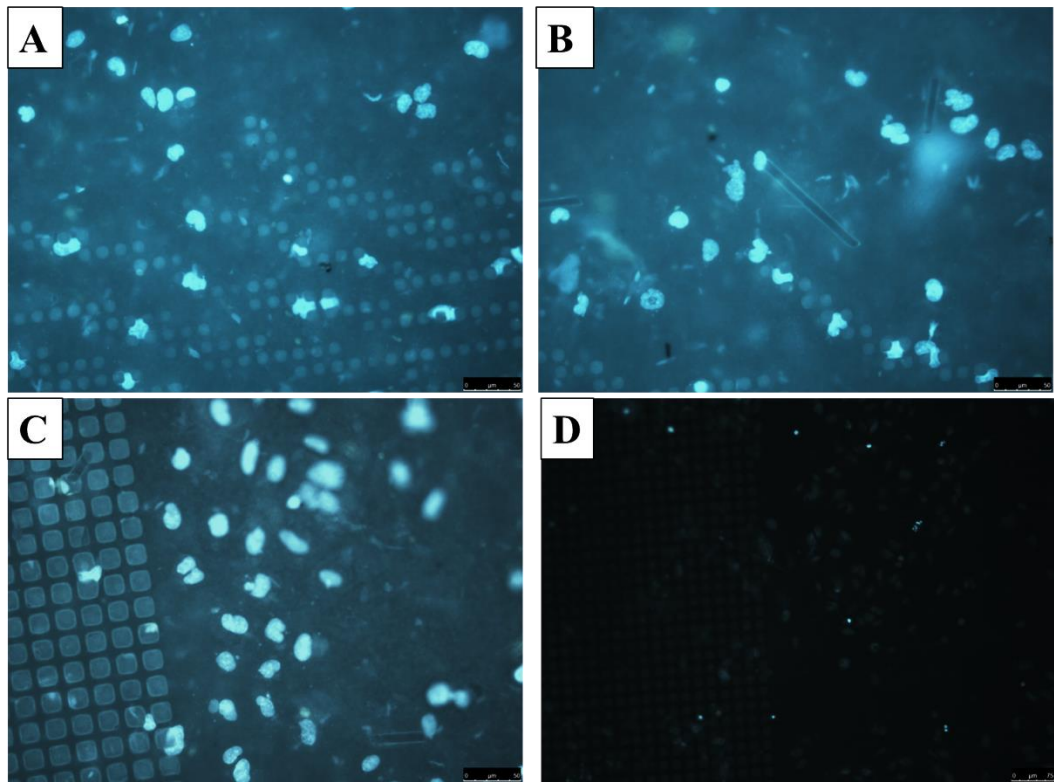
**Figure 3.14:** Saos-2 cell nuclei micrographs obtained with fluorescence microscopy on the transition region between patterned and unpatterned areas. A) and B) Pure collagen with 8x8 μm², gap 8 μm dimensions (x20), C) Pure collagen with 16x16 μm², gap 4 μm dimensions (x20), D) Collagen: ELR (1:0.1) with 8x8 μm², gap 8 μm dimensions (x10).
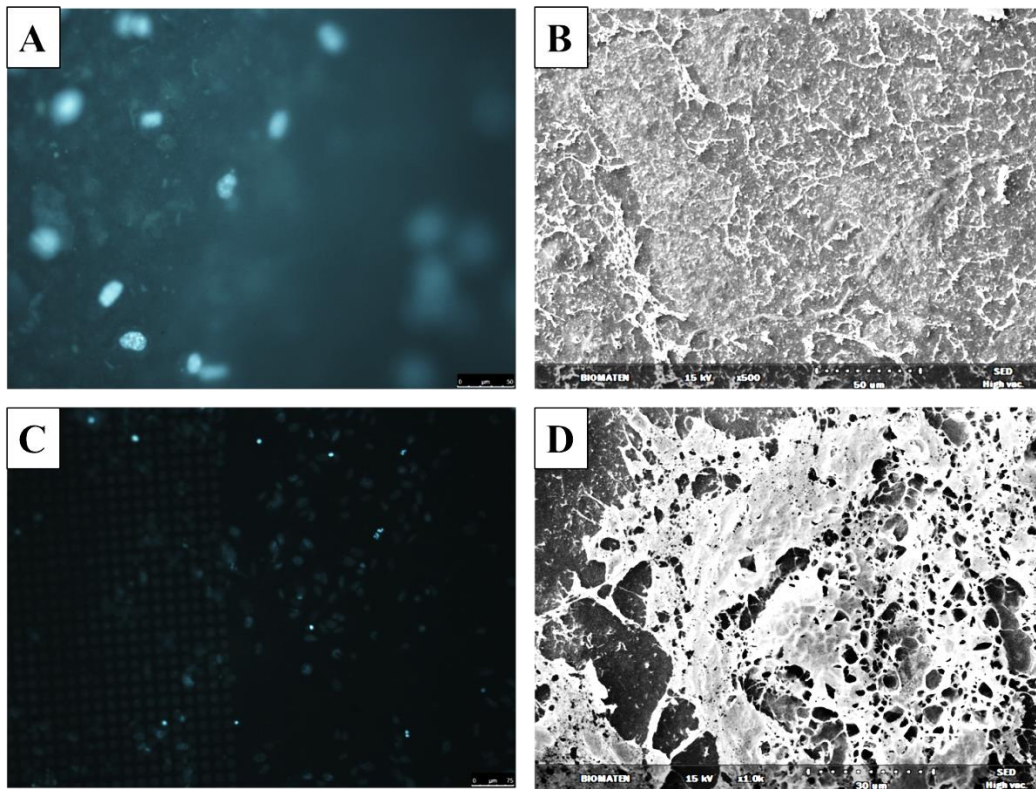
**Figure 3.15:** Saos-2 cell nuclei and cell micrographs on unpatterned surfaces. A) and C) DAPI stained nuclei micrographs with fluorescence microscope on collagen:ELR (1:0.1) surfaces (x10 and x20), B) and D) SEM micrograph of cells on collagen:ELR (1:0.1) surfaces (x500 and x1000).

All of these results show that surface topography highly affects the nucleus and cell conformation on the surfaces as many studies have shown examples of these since it was first observed (Harrison, 1912; Weiss, 1947; Curtis and Varde, 1964). After the first studies, there have been many studies and hypothesis on cell and substrate interactions. Studies involving extent of nucleus deformation with surface topography suggest that the reason of this large deformation is due to the higher flexibility and low stiffness of the cancer cells compared to healthy cells and they showed these deformations are observed much less in cancer cells (Davidson et al, 2010). This is consistent with this study that Saos-2 cell line was used which is a sarcoma cell line and they show extensive deformations on the patterned surfaces.

### 3.3.3.2 Quantification of Nucleus Deformation by Image Analysis

### 3.3.3.2.1 Frequency of Nucleus Deformation

For all surface types frequency of deformation was studied by analyzing fluorescence micrographs of the nuclei with Image J software (Rasband, 2011; Abramoff et al, 2004). For all surfaces 5 micrographs were used and ratio of deformed nuclei number to total nuclei number was found (Figure 3.16). Among all the surfaces, it can be observed that the highest deformation frequency was on the smallest pillar with largest gap. This is because the cells can take the shapes of the pillar when there is large enough space between the pillars and a small area on top of the pillars. Then the nuclei bend around the pillars. There appears to be no distinct difference between the different types of films with changing ELR contents.
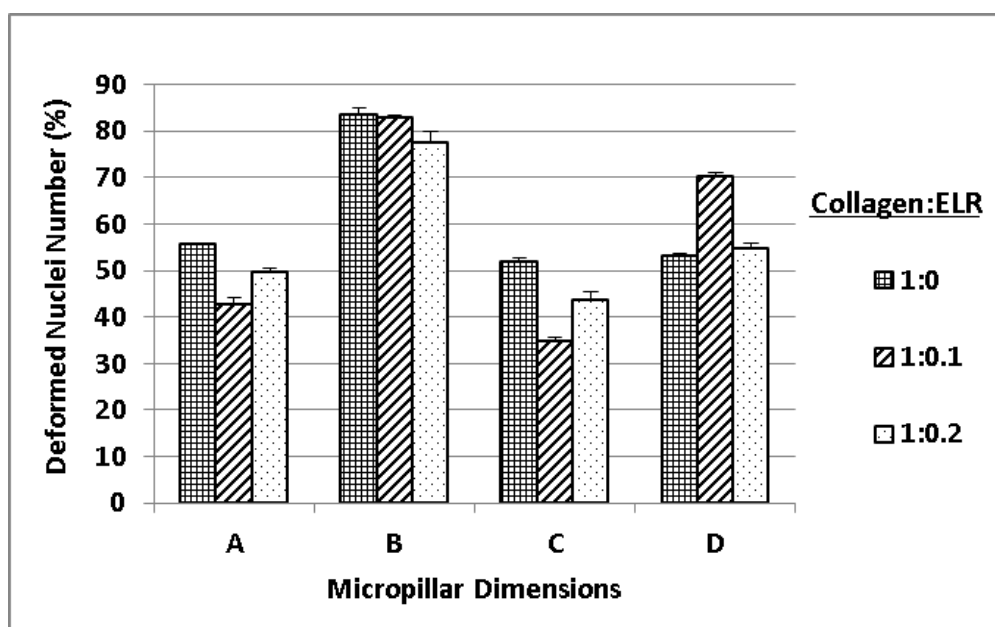


**Figure 3.16** Frequency of deformed nuclei for all types of films after 1st day of culture. A) 8x8 μm², gap 4 μm, B) 8x8 μm², gap 8 μm, C) 16x16 μm², gap 4 μm, D) 16x16 μm², gap 8 μm.

**Table 3.7** Deformed nuclei number (%) statistical analysis for pure collagen, collagen:ELR (1:0.1), collagen:ELR (1:0.2) films

| Template type | Significance compared to B |
|---|---|
| A | * |
| B | * |
| C | * |
| D | * |
| No pillar | * |

* Deformed nuclei number (%) on B area is significantly higher than the other areas (Student's t-test with a minimum confidence level of 95%, p value lower than 0.05)

### 3.3.3.2.2    Quantification of Extent of Nucleus Deformation

Another parameter used to quantify the deformation of the cell nuclei was the extent of nucleus deformation. It was found by analyzing the fluorescence microscope micrographs with Image J software (Rasband, 2011; Abramoff et al, 2004) and 5 micrographs with around 100 cells were used. Circularity was calculated according to the following equation;

**Circularity = $4\pi A / C^2$**

where A is the area of the nucleus and C is the circumference (Ferreira and Rasband, 2011). A circularity value of 1.0 indicates a perfect circle and when the value approaches 0.0, it indicates an increasingly elongated polygon. Figure 3.17 shows the circularity results obtained from the fluorescence micrographs. According to this figure, circularity of the nuclei of the cells on unpatterned films is clear. The highest deformation can be seen for the design B (8x8 $\mu$m², gap 8 $\mu$m) since this type of pillars allow the nuclei can place between the gaps and covering around the pillars with a deformation and the lowest deformation was for the unpatterned area. Cell deformation on B area was higher than the other areas but the differences were not significant for this sample size, however it can be seen significantly for the higher sample sizes. Cell deformation differences between the B area and unpatterned area was significantly different (Table 3.8). No significant difference was observed between the different film compositions as was seen in the earlier data.
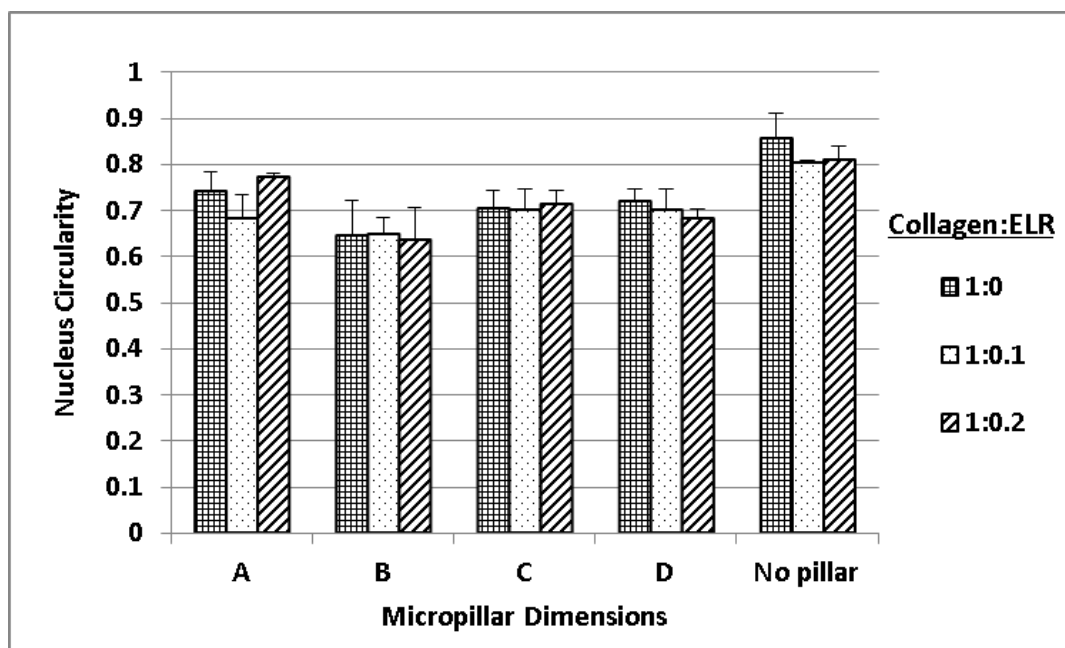
**Figure 3.17** Nucleus circularity after the 1st day of Saos-2 culture on the collagen based films. A) 8x8 μm², gap 4 μm, B) 8x8 μm², gap 8 μm, C) 16x16 μm², gap 4 μm, D) 16x16 μm², gap 8 μm.

**Table 3.8** Cell circularity statistical analysis for pure collagen, collagen:ELR (1:0.1), collagen:ELR (1:0.2) films

| Template type | Significance compared to B |
|---------------|---------------------------|
| A | - |
| B | - |
| C | - |
| D | - |
| No pillar | * |

\* Cell circularity on B area is significantly lower than the unpatterned (no pillar) area (Student's t-test with a minimum confidence level of 95%, p value lower than 0.05)

Finally, Figure 3.18 shows the perimeter of the nuclei. These results show that the highest perimeter for the nuclei was for areas having the highest pillar gaps as area B and D. These were almost same with the nuclei seeded on the unpatterned surfaces. This increase in size of the nuclei perimeter probably was due to the enough space provided by the gaps for the nuclei. Also this observation is supported with studies in the literature. In a study, endothelial cells were used with different micropillar sizes and the cells showed decreased cell areas and perimeters on fibronectin coated micropillar surfeces at the 1st day of the culture for the regions having more than 1x1 $\mu m^2$ sizes (Dickinson et al, 2012). Finally, no significant difference was observed between the different film compositions as was seen in the earlier data.
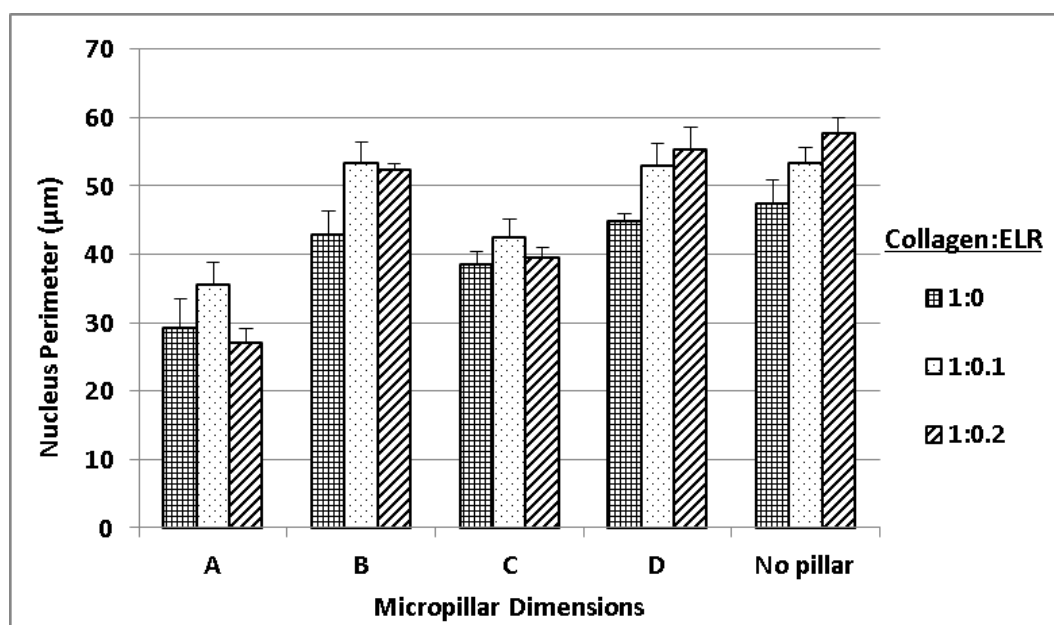


**Figure 3.18** Nucleus perimeter after the 1st day of Saos-2 culture on the collagen based films. A) 8x8 μm², gap 4 μm, B) 8x8 μm², gap 8 μm, C) 16x16 μm², gap 4 μm, D) 16x16 μm², gap 8 μm.

**Table 3.9** Cell perimeter analysis for pure collagen, collagen:ELR (1:0.1), collagen:ELR (1:0.2) films

| Template type | Significance compared to B | Significance compared to D | Significance compared to no pillar |
|---|---|---|---|
| A | * | ** | *** |
| B | - | - | - |
| C | * | ** | *** |
| D | - | - | - |
| No pillar | - | - | - |

* Cell perimeter on B area is significantly higher than the others (Student's t-test with a minimum confidence level of 95%, p value lower than 0.05)

** Cell perimeter on D area is significantly higher than the others (Student's t-test with a minimum confidence level of 95%, p value lower than 0.05)

*** Cell perimeter on unpatterned (no pillar) area is significantly higher than the others (Student's t-test with a minimum confidence level of 95%, p value lower than 0.05)

# CHAPTER 4

## CONCLUSION AND FUTURE STUDIES

Cell and substrate interactions are important in tissue engineering products and behavior of the cells such as proliferation, adhesion, migration, and differentiation have been widely studied on the substrates with different physical, chemical, mechanical properties and shape. In this study, ELR and collagen based films with micropillar surface topographies are used to study for further observations of cell-substrate interactions. Nucleus and cell deformations were observed for all type of films in terms of adhesion, proliferation and conformational change. However the effect of ELR composition was not seen in terms of adhesion, proliferation and conformational change in the results whereas ELR content was highly effective on the ALP activity. On the other hand, micropillar dimensions were found to be very effective on adhesion, ALP activity and conformational change.

For further improvements of this study, ELR composition may be increased to see the effect of ELR content on cell adhesion, proliferation and conformational change. Also, focal adhesion points of the cells onto the micropillars can be observed by staining extracellular elements of the cells besides the nucleus. Moreover, an improved crosslinking should be tried for the films composing ELR and collagen since the films swelled after 14 days. Finally, a new design of films before cell seeding for the in vitro studies can be considered in order to avoid the deviations in cell numbers since the cells mostly flow from the film surfaces during the seeding procedure.

# REFERENCES

Abràmoff MD, Magalhães PJ, Ram SJ. Image Processing with ImageJ. Biophotonics International. 2004; 11(7):36–42.

Agaska B, Bacakova L, Filova E, Balik K. Osteogenic cells on bio-inspired materials for bone tissue engineering. Physiological Research. 2010; 59:309-322.

Agrawal CM. Reconstructing the human body using biomaterials. JOM. 1998; 31–35.
Alberts B, Bray D, Lewis J, Raff M, Roberts K, Watson JD. Molecular biology of the cell. 3rd Edition. New York:Garland Publishing Inc. 1994.

Allen LT, Tosetto M, Miller IS, O'Connor DP, Penney SC, Lynch I. Surface-induced changes in protein adsorption and implications for cellular phenotypic responses to surface interaction. Biomaterials. 2006; 27:3096-3108.

Andersson AS, Backhed F, VonEuler A, Richter-Dahlfors A, Sutherland D, Kasemo B. Nanoscale features influence epithelial cell morphology and cytokine production. Biomaterials. 2003; 24:3427-3436.

Arias FJ, Reboto V, Martin S, Lopez I, Rodriguez-Cabello JC. Tailored recombinant elastin-like polymers for advanced biomedical and nano(bio)technological applications. Biotechnol Lett. 2006; 28:687-695.

Badique F, Stamov DR, Davidson PM, Veuillet M, Reiter G, Freund JN, Franz CM, Anselme K. Directing nuclear deformation on micropillared surfaces by substrate geometry and cytoskeleton organization. Biomaterials. 2013; 1-11.

Bauer AL, Jackson TL, Jiang Y. Topography of extracellular matrix mediates vascular morphogenesis and migration speeds in angiogenesis. PLoS computational biology. 2009; 5:1553-7358.

Benayahu D, Shur I, Marom R, Meller I, Issakov J. Cellular and Molecular Properties Associated With Osteosarcoma Cells Journal of Cellular Biochemistry. 2002; 84:108-114.

Ber S, Kose GT, Hasirci V, Bone tissue engineering on patterned collagen films: An in vitro study. Biomaterials. 2005; 26:1977-1986.

Berkowski K, Plunkett KN, Yuand Q, Moore JS. Introduction to photolithography: Preparation of microscale polymer silhouettes. Journal of Chemical Education. 2005; 82:1365-1369.

Bet MR, Goissis G, Vargas S, Selistre-de-Araujo HS. Cell adhesion and cytotoxicity studies over polyanionic collagen surfaces with variable negative charge and wettability. Biomaterials. 2003; 24:131-137.

Bettinger CJ, Langer R, Borenstein JT. Engineering substrate micro- and nanotopography to control cell function. Angew Chem Int Ed Engl. 2009; 48: 5406-5415.

Bettinger CJ, Zhang Z, Gerecht S, Borenstein JT, Langer R. Enhancement of In Vitro Capillary Tube Formation by Substrate Nanotopography. Adv Mater. 2008; 20:99-103.

Biggs M, Richards R, Gadegaard N, Wilkinson C, Dalby M. The effects of nanoscale pits on primary human osteoblast adhesion formation and cellular spreading. J Mater Sci-Mater M. 2007; 18:399-404.

Bilbe G, Roberts E, Birch M, Evans DB. PCR phenotyping of cytokines, growth factors and their receptors and bone matrix proteins in human osteoblast-like cell lines. Bone. 1996; 19:437-445.

Billiet T, Vandenhaute M, Schelfhout J, Van VS, Dubruel P. A review of trends and limitations in hydrogel-rapid prototyping for tissue engineering. Biomaterials. 2012; 33:6020-6041.

Bou-Gharios G, de Crombrugghe B. Chapter 15 - type I collagen structure, synthesis, and regulation. In: Bilezikian JP, Raisz LG, Martin TJ, editors. Principles of bone biology. 3rd ed. San Diego: Academic Press, 2008; 285-318.

Burg KJL, Porter S, Kellam JF. Biomaterials development for bone tissue engineering. Biomaterials. 2000; 21:2347-2359.

Caille N, Thoumine O, Tardy Y, Meister JJ. Contribution of the nucleus to the mechanical properties of endothelial cells. Journal of Biomechanics. 2002; 35:177–187.

Chauvy PF, Hoffmann P, Landolt D. Applications of laser lithography on oxide film to titanium micromachining. Applied Surface Science. 2003; 165-170.

Cheema U, Ananta M, Mudera V. Collagen applications of a natural polymer. In: Eberli D, editor. Regenerative Medicine and Tissue Engineering - Cells and biomaterials. InTech, 2011.

Chen Y, Pe´pin A. Nanofabrication:conventional and nonconventionalmethods. Electrophoresis. 2001; 22:187–207.

Chilkoti A., Christensen T., MacKay J.A. Stimulus responsive elastin biopolymers: Applications in medicine and biotechnology. Curr Opin Chem Biol. 2006; 10: 652-7.

Clarke MSF, Feeback DL. Mechanical load induces sarcoplasmic wounding and FGF release in differentiated human skeletal muscle cultures. FASEB Journal. 1996; 10:502–509.

Costa RR, Custo´dio CA, Testera AM, Arias FJ, Rodriguez-Cabello JC, Alves NM, Mano JF. Stimuli responsive thin coatings using elastin-like polymers for biomedical applications. Adv. funct. Mater. 2009; 19, 3210–3218.

Coutinho D, Costa P, Neves N, Gomes ME, Reis RL. Micro- and nanotechnology in tissue engineering. In: Pallua N, Suschek CV, editors. Berlin Heidelberg: Springer. 2011; 3-29.

Curtis AS, Varde M. Control of cell behavior: topological factors. J. Natl. Cancer Inst. 1964; 33:15–26.

Curtis ASG, Dalby M, Gadegaard N. Cell signaling arising from nanotopography: implications for nanomedical devices. Nanomedicine. 2006; 1: 67-72.

Cytoo, Adhesive Micropatterns-CYTOO cell architects, http://www.cytoo.com/, 2013.

Dalby MJ, Gadegaard N,Tare R, Andar A, Riehle MO, Herzyk P,Wilkinson, CDW, Oreffo ROC. The control of human mesenchymal cell differentiation using nanoscale symmetry and disorder. Nat.Mater. 2007; 6:997–1003.

Dalby MJ, McCloy D, Robertson M, Agheli H, Sutherland D, Affrossman S, Oreffo ROC. Osteoprogenitor response to semi-ordered and random nanotopographies. Biomaterials. 2006; 27:2980–2987.

Dalby MJ, Riehle MO, Johnstone H, Affrossman S, Curtis ASG. In vitro reaction of endothelial cells to polymer demixed nanotopography. Biomaterials. 2002; 23:2945–2954.

Dalby MJ, Riehle MO, Sutherland DS, Agheli H, Curtis ASG. Fibroblast response to a controlled nanoenvironment produced by colloidal lithography. J. Biomed. Mater. Res. 2004; 69:314–322.

Dalton BA, Walboomers F, Dziegielewski M, Evans MDM, Taylor S, Jansen JA, Steele JG. Modulation of epithelial tissue and cell migration by microgrooves. J Biomed Mater Res. 2001; 56:195-207.

Davidson PM, Fromigue O, Marie PJ, Hasirci V, Reiter G, Anselme K. Topographically induced self-deformation of the nuclei of cells: dependence on cell type and proposed mechanisms. J Mater Sci: Mater Med. 2010; 21:939–946.

Davidson PM, Ozcelik H, Hasirci V, Reiter G, Anselme K. Microstructured surfaces cause severe but non-detrimental deformation of the cell nucleus. Adv. Mater. 2009; 21:3586–3590.

Deguchi S, Maeda K, Ohashi T, Sato M. Flow-induced hardening of endothelial nucleus as an intracellular stress-bearing organelle. J. Biomech. 2005; 38:1751.

Dickinson LE, Rand DR, Tsao J, Eberle W, Gerecht S. Endothelial cell responses to micropillar substrates of varying dimensions and stiffness. J Biomed Mater Res. 2012; 100: 1457–1466.

Dong C, Skalak R, Sung KL. Cytoplasmic rheology of passive neutrophils. Biorheology. 1991; 28:557-567.

Donoso MG, Mendez-Vilas A, Bruque JM, Gonzalez-Martin ML. On the relationship between common amplitude surface roughness parameters and surface area: Implications for the study of cell–material interactions. International Biodeterioration and Biodegradation. 2007; 59:245-251.

Dunn GA, Brown AF. Alignment of fibroblasts on grooved surfaces described by a simple geometric transformation. J. Cell Sci. 1986; 83:313–340.

Fernandes RJ, Harkey MA, Weis M, Askew JW, Eyre DR. The post-translational phenotype of collagen synthesized by SAOS-2 osteosarcoma cells. Bone. 2007; 40:1343-1351.

Ferreira T and Rasband W. The ImageJ User Guide — Version 1.44, http://imagej.nih.gov/ij/docs/user-guide.pdf, 2011.

Franke H, Galla H, and Beuckmann CT Primary cultures of brain microvessel endothelial cells: a valid and flexible model to study drug transport through the blood-brain barrier in vitro. Brain Res Brain Res Protoc. 2000; 5:248-256.

Frenette J, Tidball JG. Mechanical loading regulates expression of talin and its mRNA, which are concentrated at myotendinous junctions. American Journal of Physiology. 1998; 275:818-825.

Fu J, Wang YK, Yang MT, Desai RA, Yu X, Liu Z, Chen SC. Mechanical regulation of cell function with geometrically modulated elastomeric substrates. Nature Methods. 2010.

Fullana MJ, Wnek GE. Electrospun collagen and its applications in regenerative medicine. Drug Delivery and Translational Research. 2012; 2:313-322.

Gallagher JO, McGhee KF, Wilkinson CDW, Riehle MO. Interaction of animal cells with ordered nanotopography. Nanobiosci. 2002; 1:24–28.

Gauvin R, Chen YC, Lee JW, Soman P, Zorlutuna P, Nichol JW, Bae H, Chen S,Khademhosseini A. Microfabrication of complex porous tissue engineering scaffolds using 3D projection stereolithography. Biomaterials. 2012; 33:3824-3834.

Gelsea K, Poschl E, Aigner T. Collagens-structure, function, and biosynthesis. Advanced Drug Delivery Reviews. 2003; 55:1531-1546.

Gerecht S,Bettinger CJ, Zhangc Z, Borensteind JT,Vunjak Novakovice G, Langer R. The effect of actin disrupting agents on contact guidance of human embryonic stem cells. Biomaterials. 2007; 28:4068-4077.

Goddard JM, Hotchkiss JH. Polymer surface modification for the attachment of bioactive compounds. Progress in Polymer Science. 2007; 32: 698-725.

Goldman RD, Clement S, Khuon S, Moir R, Trejo-Skalli A, Spann T, Yoon M. Intermediate filament cytoskeletal system: dynamic and mechanical properties. Biological Bulletin. 1998; 194:361–363.

Goldman RD, Khuon S, Chou YH, Opal P, Steinert P. The function of intermediate filaments in cell shape and cytoskeletal integrity. Journal of Cell Biology. 1996; 134: 971–983.

Green AM, Jansen JA, venderWaerden JPCM, von Recum AF. Fibroblast response to microtextured silicone surfaces: texture orientation in toor out of the surface. J. Biomed. Mater. Res. 1994; 28:647–653.

Guilak F, Tedrow JR, Burgkart R. Viscoelastic properties of the cell nucleus. Biochemical and Biophysical Research Communications. 2000; 269:781–786.

Gunatillake PA, Adhikari R.Biodegradabla synthetic polymers for tissue engineering. European Cells and Materials. 2003; 5:1-16.

Ha TLB, Quan TM, Vu DN, Si DM. Naturally derived biomaterials: Preparation and application. In: Andrades JA, editor. Regenerative Medicine and Tissue Engineering. InTech, 2013.

Harrison RG. The cultivation of tissues in extraneous medium as a method of morphogenetic study. Anat. Rec. 1912; 6:181–93.

Hart A, Gadegaard N, Wilkinson C, Oreffo R, Dalby M. Osteoprogenitor response to low-adhesion nanotopographies originally fabricated by electron beam lithography. J Mater Sci-Mater M. 2007; 18:1211-1218.

Hasirci V, Kenar H. Novel surface patterning approaches for tissue engineering and their effect on cell behavior. Nanomedicine. 2006; 1:73-90.

Hatano K, Inoue H, Kojo T, Tsujisawa T, Uchiyama C, Uchida Y. Effect of surface roughness on proliferation and alkaline phosphatase expression of rat calvarial cells cultured on polystyrene. Bone. 1999; 25:439-445.

Hoffmann K, Sperling K, Olins AL, Olins DE. The granulocyte nucleus and lamin B receptor: avoiding the ovoid. Chromosoma. 2007; 116:227–235.

Hollinger JO. Preliminary report on osteogenic potential of a biodegradable copolymer of polylactide (PLA) and polyglycolide (PGA). J Biomed Mater Res. 1983; 17:71-82.

Hsu SH, Chen CY, Lu PS, Lai CS, Chen CJ. Oriented Schwann cell growth on microgrooved surfaces. Biotechnol Bioeng. 2005; 92:579-588.

Huebsch N, Arany PR, Mao AS, Shvartsman D, Ali OA, Bencherif SA, Rivera-Feliciano J, Mooney DJ. Harnessing traction-mediated manipulation of the cell/matrix interface to control stem-cell fate. Nature materials. 2010; 9:518-526.

Hunt JA,Williams RL,Tavakoli SM, Riches ST. Laser surface modification of polymers to improve biocompatibility. J.Mater.Sci.Mater.Med. 1995; 6:813–817.

Hutmacher DW. Scaffold design and fabrication technologies for engineering tissues--state of the art and future perspectives. Journal of biomaterials science. 2001; 12:107-124.

Hynes RO. The extracellular matrix: not just pretty fibrils. Science. 2009; 326:1216-1219.

Ishikawa J, Tsuji H, Sato H, Gotoh Y. Ion implantation of negative ions for cell growth manipulation and nervous system repair. Surface and coatings technology. 2007; 201: 8083-8090.

Janmey PA, Euteneuer U, Traub P, Schliwa M. Viscoelastic properties of vimentin compared with other filamentous biopolymer networks. Journal of Cell Biology. 1991; 113:155–160.

Janmey PA. The cytoskeleton and cell signaling: component localization and mechanical coupling. Physiological Reviews. 1998; 78:763-781.

Karageorgiou V, Kaplan D. Porosity of 3D biomaterial scaffolds and oseogenesis. Biomaterials. 2005; 26:5474-5491.

Karnovsky, MJ. A formaldehyde-glutaraldehyde fixative of high osmolarity for use in electron microscopy. J. Cell Biol. 1965; 27:137.

Keselowsky BG, Collard DM, García AJ. Integrin binding specificity regulates biomaterial surface chemistry effects on cell differentiation. Proc Natl Acad Sci. 2005; 102:5953-5957.

Kim BS, Mooney DJ. Development of biocompatible synthetic extracellular matrices for tissue engineering. TIBTECH. 1998; 16: 224-230.

Kinikoglu B, Rodriguez-Cabello JC, Damour O, Hasirci V. A smart bilayer scaffold of elastin-like recombinamer and collagen for soft tissue engineering. J Mater Sci: Mater Med. 2011; 22:1541-1554.

Kohn J, Langer R. Bioresorbable and bioerodible materials. In: Ratner BD, Hoffman AS, Schoen FJ, Lemon JE, editors. An Introduction to Materials in Medicine. San Diego:Academic Press, 1997; 65-73.

Lauffenburger DA, Linderman JJ. Receptors: Models for binding, trafficking, and signaling. 1993.

Lee JH, Jung HW, Kang IK, Lee HB. Cell behaviour on polymer surfaces with different functional groups. Biomaterials. 1994; 15:705-711.

Lenhert S, Meier M-B, Meyer U, Chi L, Wiesmann HP. Biomaterials. Osteoblast alignment, elongation and migration on grooved polystyrene surfaces patterned by Langmuir-Blodgett lithography. 2005; 26:563-570.

Levental KR, Yu H, Kass L, Lakins JN, Egeblad M, Erler JT, Fong SF, Csiszar K, Giaccia A, Weninger W, Yamauchi M, Gasser DL, Weaver VM. Matrix crosslinking forces tumor progression by enhancing integrin signaling. Cell. 2009; 139: 891-906.

Lim JY, Hansen JC, Siedlecki CA, Runt J, Donahue HJ. Human foetal osteoblastic cell response to polymer-demixed nanotopographic interfaces. Journal of Royal Society Interface. 2005; 2:97-108.

Lin CY, Li LT, Su WT. Study of subcellular dynamics on cell–substrate interactions by live cell imaging. J Biomed Mater Res. 2013.

Liu W, Chen Z, Jiang X. Methods for cell micropatterning on two-dimensional surfaces and their applications in biology. Chin J Anal Chem. 2009; 37: 943–949.

Loesberg WA, te Riet J, van Delft FC, Schön P, Figdor CG, Speller S, van Loon JJ, Walboomers XF, Jansen JA. The threshold at which substrate nanogroove dimensions may influence fibroblast alignment and adhesion. Biomaterials. 2007; 28:3944-3951.

Luna EJ, Hitt AL. Cytoskeleton-plasma membrane interactions. Science. 1992; 258:955-963.
Maniotis AJ, Chien CS, Ingber DE. Demonstration of mechanical connections between integrins, cytoskeletal filaments, and nucleoplasm that stabilize nuclear structure. Proceedings of the National Academy of Sciences. 1997; 94:849-854.

Martinez E, Engel E, Planell JA, Samitier J. Effects of artificial micro- and nano-structured surfaces on cell behaviour. Ann Anat. 2009; 191:126-135.

Matsuzaka K,Walboomers XF,Yoshinari M, Inoue T, Jansen  JA. The attachment and growth behavior of osteoblast-like cells on microtextured surfaces. Biomaterials. 2003; 24:2711–2719.

McMurray R, Dalby MJ, Gadegaard N. Nanopatterned surfaces for biomedical applications. In: Laskovski A, editor. Biomedical Engineering Trends in Materials Science. 2011.

Miller D., Thapa A, Habestroh KM, Webster TJ. Endothelial and vascular smooth cell function on poly(lactic-co-glycolic acid) with nano structured surface features. Biomaterials. 2004; 25:53–61.

Mol A, Bouten CV, Zund G, Gunter CI, Visjager JF, Turina MI, Baaijens FP, Hoerstrup SP. The relevance of large strains in functional tissue engineering of heart valves. The Thoracic and Cardiovascular Surgeon. 2003; 51:78–83.

Nelson JF, Stanford HG, Cutright DE. Evaluation and comparison of biodegradable substances as osteogenic agents. Oral Surg. 1977; 43:836-843.

Nguyen N. Micromixers: Fundamentals, design and fabrication. In: Andrew W, editor. Applied Science Publishers. 2008; 79-134.

O'Brien FJ. Biomaterials and scaffolds for tissue engineering. Materials Today. 2011; 14.
Pan Z, Yan C, Peng R, Zhao Y, He Y, Ding J. Control of cell nucleus shapes via micropillar patterns. Biomaterials. 2012; 33:1730-1735.

Parviz BA, Ryan D, George M. Using Self-Assembly for the Fabrication of Nano-Scale Electronic and Photonic Devices. IEEE Transactions on Advanced Packaging. 2003; 26.

Patra S. Design and Modeling of Axial Micro GasTurbine. Bachelors of Technology Thesis, National Institute of Technology (NIT),  Department of Mechanical Engineering, Rourkela, India, 2010.

Pauetki C, Schieker M, Tischer T, Kolk A, Neth P, Mutschler W, Milz S. Characterization of osteosarcoma cell lines MG-63, Saos-2 and U-2 OS in comparison to human osteoblasts. Anticancer Research. 2004; 24: 3743-3748.

Popat KC, Chatvanichkul KI, Barnes GL, Latempa Jr. TJ, Grimes CA, Desai TA. Osteogenic differentiation of marrow stromal cells cultured on nanoporous alumina surfaces. J.Biomed.Mater.Res. 2007; 80:955–964.

Rajnicek AM, Foubister LE, McCaig CD. Prioritising guidance cues: directional migration induced by substratum contours and electrical gradients is controlled by a rho/cdc42 switch. Dev Biol. 2007; 312:448-460.

Rasband WS. ImageJ, U.S. National Institutes of Health, Bethesda, Maryland, USA, http://imagej.nih.gov/ij/, 2011.

Rodan SB, Imai Y, Thiede MA, Wesolowski G, Thompson D, Bar-Shavit Z, Shull S, Mann K, Rodan GA. Characterization of a human osteosarcoma cell line (Saos-2) with osteoblastic properties. Cancer Res. 1987; 47:4961-4966.

Rodriguez-Cabello JC, Martin L, Alonso M, Arias FJ, Testera AM. Recombinamers as advanced materials for the post-oil age. Polymer. 2009; 50:5159-5169.

Rowat AC, Lammerding J, Herrmann H, Aebi U. Towards an integrated understanding of the structure and mechanics of the cell nucleus. BioEssays. 2008; 30:226-236.

Saldana L, Bensiamar F, Bore A, Vilaboa N. In search of representative models of human bone-forming cells for cytocompatibility studies. Acta Biomater. 2011; 7:4210- 4221.

Santos E, Orive G, Hernández RM, Pedraz JL. Cell-Biomaterial Interaction: Strategies To Mimic The Extracellular Matrix. In: Pramatarova L , editor. Biomimetics. InTech. 2011.

Schneider GB, English A, Abraham M, Zaharias R, Stanford C, Keller J. The effect of hydrogel charge density on cell attachment. Biomaterials. 2004; 25:3023- 3028.

Sell SA, Wolfe PS, Garg K, McCool JM, Rodriguez IA, Bowlin GL. The Use of Natural Polymers in Tissue Engineering: A Focus on Electrospun Extracellular Matrix Analogues. Polymers. 2010; 2:522-553.

Shimi T, Butin-Israeli V, Goldman RD. The functions of the nuclear envelope in mediating the molecular crosstalk between the nucleus and the cytoplasm. Current Opinion in Cell Biology. 2012; 24:71-78.

Stein GS, Lian JB. Molecular mechanisms mediating proliferation/ differentiation interrelationships during progressive development of the osteoblast phenotype. Endocrine Reviews. 1993; 14:424-441.

Stuurman N, Heins S, Aebi U. Nuclear lamins: their structure, assembly and interactions. Journal of Structural Biology. 1998; 122:42–66.

Subramani, K. Fabrication of hydrogel micropatterns by soft photolithography. In: Ahmed W, Jackson JM, editors. Emerging nanotechnologies for manufacturing. Elsevier. 2009; 261-276.

Suresh S. Biomechanics and biophysics of cancer cells. Acta Materialia. 2007; 55:3989–4014.

Tamada Y, Ikada Q. Effect of preadsorbed proteins on cell adhesion to polymer surfaces. Journal of Colloid and Interface Science. 1993; 155: 334-339.

Tek P, Chiganos TC, Mohammed JS, Eddington DT, Fall CP, Ifft P, Rousche P J. Rapid prototyping for neuroscience and neural engineering. Journal of Neuroscience Methods. 2008; 172:263-269.

Thery M, Jiménez-Dalmaroni A, Racine V, Bornens M, Jülicher F. Experimental and theoretical study of mitotic spindle orientation. Nature. 2007; 447:493-496.

Thery M, Pépin A, Dressaire E, Chen Y, Bornens M. Cell distribution of stress fibres in response to the geometry of the adhesive environment. Cell Motil. Cytoskeleton. 2006b; 63: 341-355.

Thery M, Racine V, Pépin A, Piel M, Chen Y, Sibarita JB, Bornens M. The extracellular matrix guides the orientation of the cell division axis. Nature Cell Biology. 2005; 7:947-953.

Thery M, Racine V, Piel M, Pépin A, Dimitrov A, Chen Y, Sibarita JB, Bornens M. Anisotropy of cell adhesive microenvironment governs cell internal organization and orientation of polarity. PNAS. 2006a; 103:19771-19776.

Tseng Q, Wang I, Duchemin-Pelletier E, Azioune A, Carpi N, Gao J, Filhol O, Piel M, Thery M, Balland M. A new micropatterning method of soft substrates reveals that different tumorigenic signals can promote or reduce cell contraction levels. The Royal Society of Chemistry. 2011.

Tzvetkova-Chevolleau T, Stéphanou A, Fuard D, Ohayon J, Schiavone P, Tracqui P. The motility of normal and cancer cells in response to the combined influence of the substrate rigidity and anisotropic microstructure. Biomaterials. 2008; 29:1541-1551.

Upcraft S, Fletcher R. The rapid prototyping technologies. Assembly Automation. 2003; 23:318-330.

Vandenburgh HH. Mechanical forces and their second messengers in stimulating cell growth in vitro. American Journal of Physiology. 1992; 262:350-355.

Voldman J, Gray ML, Schmidt MA. Microfabrication in biology andmedicine. Annu. Rev. Biomed. Eng. 1999; 1:401–25.

Wang L, Carrier RB. Biomimetic Topography: Bioinspired Cell Culture Substrates and Scaffolds, In: Cavrak M, editor. Advances in Biomimetics. InTech. 2011.

Wang X, Ohlin CA, Lu Q, Hu J. Biomaterials. Cell directional migration and oriented division on three-dimensional laser-induced periodic surface structures on polystyrene. 2008; 29:2049-2059.

Wei J, Igarashi T, Okumori N, Maetani T, Liu BS, Yoshinari M. Influence of surface wettability on competitive protein adsorption and initial attachment of osteoblasts. Biomedical Materials. 2009; 4.

Weiss P. The problem of specificity in growth and development. Yale J. Biol. Med. 1947; 19:235–78.

Wojciak-Stothard B, Madeja Z, Korohoda W, Curtis A, Wilkinson C. Activation of macrophage-like cells by multiple grooved substrata.Topographical control of cell behavior. CellBiol.Int. 1995; 19:485-490.

Wuthier RE. A review of the primary mechanism of endochondral calcification with special emphasis on the role of cells, mitochondria and matrix vesicles. Clin Orthop Rel Res. 1982; 169: 219-42.

Xu LC. Effect of surface wettability and contact time on protein adhesion to biomaterial surfaces. Biomaterials. 2007; 28: 3273-3283.

Yamada KM, Miyamato S. Integrin transmembrane signaling and cytoskeletal control. Current Opinion in Cell Biology. 1995; 7:681-689.

Yang S, Leong K, Du F, Chua Z., C. K. The design of scaffolds for use in tissue engineering: Rapid prototyping techniques. Tissue Engineering. 2002;8.

Yeung T, Georges PC, Flanagan LA, Marg B, Ortiz M. Effects of substrate stiffness on cell morphology, cytoskeletal structure, and adhesion. Cell Motil Cytoskeleton. 2005; 60:24-34.

Yim EKF, Pang SW, Leong KW.  Synthetic nanostructures inducing differentiation of human mesenchymal stem cells into neuronal lineage. Exp Cell Res. 2007; 313:1820-1829.

Yim EKF, Reano RM, Pang SW, Yee AF, Chen CS, Leong KW. Biomaterials. Nanopattern-induced changes in morphology and motility of smooth muscle cells. 2005; 26:5405-5413.

Yolanda G, Hemantkumar N, Collighan R, Griffin M, Rodriguez-Cabello JC, Pandit A. In vitro characterization of a collagen scaffold enzymatically cross-linked with a tailored elastin-like polymer. Tissue Engineering. 2009; 15.

Zhang S. Fabrication of novel biomaterials through molecular self-assembly. Nature Biotechnology. 2003; 21.

Zhu C, Bao G, Wang N. Cell mechanics: mechanical response, cell adhesion, and molecular deformation. Annual Review of Biomedical Engineering. 2000; 2:189-226.

Zorlutuna P, Elsheikh A, Hasirci V. Nanopatterning of Collagen scaffolds improve the mechanical properties of tissue engineered vascular grafts. Biomacromolecules. 2009; 10:814-821.

**STANDARD CURVE FOR ALP ASSAY**
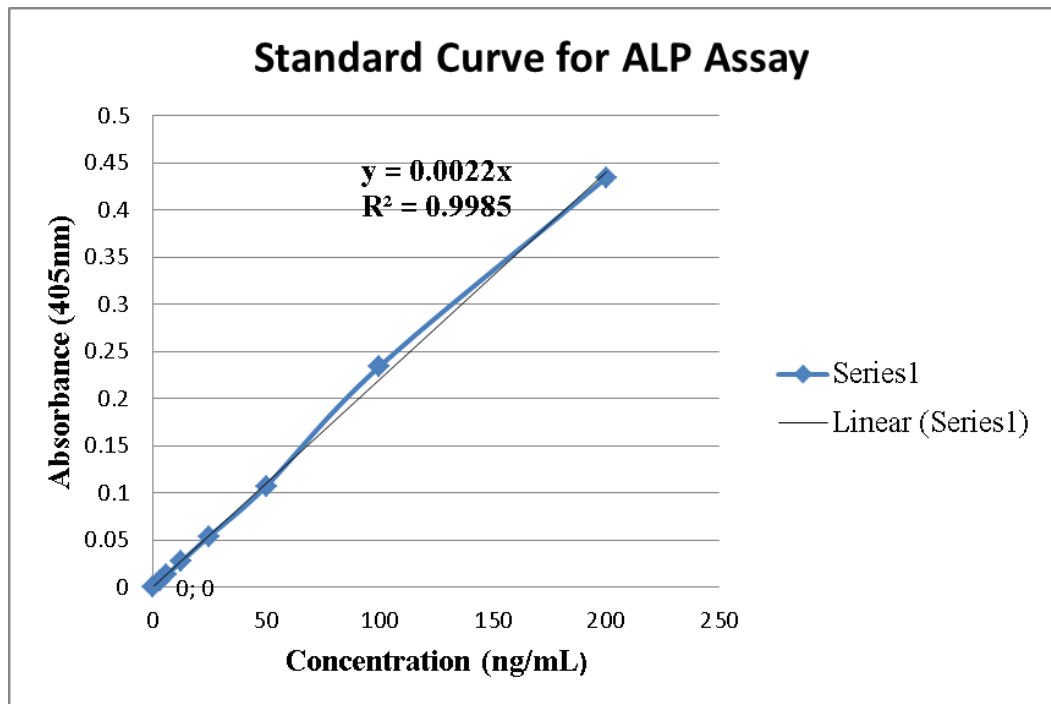


**Figure A1:** Standard curve for ALP essay